

# PROCEEDINGS OF SPIE

## ***Infrared Technology and Applications XXXVIII***

**Bjørn F. Andresen  
Gabor F. Fulop  
Paul R. Norton**  
*Editors*

**23–27 April 2012  
Baltimore, Maryland, United States**

*Sponsored and Published by*  
SPIE

**Volume 8353**  
Part One of Two Parts

Proceedings of SPIE, 0277-786X, v. 8353

SPIE is an international society advancing an interdisciplinary approach to the science and application of light.

Infrared Technology and Applications XXXVIII, edited by Bjørn F. Andresen, Gabor F. Fulop, Paul R. Norton,  
Proc. of SPIE Vol. 8353, 835301 · © 2012 SPIE · CCC code: 0277-786X/12/\$18 · doi: 10.1117/12.934826

The papers included in this volume were part of the technical conference cited on the cover and title page. Papers were selected and subject to review by the editors and conference program committee. Some conference presentations may not be available for publication. The papers published in these proceedings reflect the work and thoughts of the authors and are published herein as submitted. The publisher is not responsible for the validity of the information or for any outcomes resulting from reliance thereon.

Please use the following format to cite material from this book:

Author(s), "Title of Paper," in *Infrared Technology and Applications XXXVIII*, edited by Bjørn F. Andresen, Gabor F. Fulop, Paul R. Norton, Proceedings of SPIE Vol. 8353 (SPIE, Bellingham, WA, 2012) Article CID Number.

ISSN 0277-786X  
ISBN 9780819490315

Published by

**SPIE**

P.O. Box 10, Bellingham, Washington 98227-0010 USA  
Telephone +1 360 676 3290 (Pacific Time) · Fax +1 360 647 1445  
SPIE.org

Copyright © 2012, Society of Photo-Optical Instrumentation Engineers

Copying of material in this book for internal or personal use, or for the internal or personal use of specific clients, beyond the fair use provisions granted by the U.S. Copyright Law is authorized by SPIE subject to payment of copying fees. The Transactional Reporting Service base fee for this volume is \$18.00 per article (or portion thereof), which should be paid directly to the Copyright Clearance Center (CCC), 222 Rosewood Drive, Danvers, MA 01923. Payment may also be made electronically through CCC Online at [copyright.com](http://copyright.com). Other copying for republication, resale, advertising or promotion, or any form of systematic or multiple reproduction of any material in this book is prohibited except with permission in writing from the publisher. The CCC fee code is 0277-786X/12/\$18.00.

Printed in the United States of America.

Publication of record for individual papers is online in the SPIE Digital Library.

The logo for SPIE Digital Library features the word "SPIE" in a bold, sans-serif font above the words "Digital Library" in a smaller, lighter font. To the right of the text is a stylized graphic consisting of three vertical bars of increasing height from left to right, with a curved line above them.

[SPIDigitalLibrary.org](http://SPIDigitalLibrary.org)

---

**Paper Numbering:** Proceedings of SPIE follow an e-First publication model, with papers published first online and then in print and on CD-ROM. Papers are published as they are submitted and meet publication criteria. A unique, consistent, permanent citation identifier (CID) number is assigned to each article at the time of the first publication. Utilization of CIDs allows articles to be fully citable as soon as they are published online, and connects the same identifier to all online, print, and electronic versions of the publication. SPIE uses a six-digit CID article numbering system in which:

- The first four digits correspond to the SPIE volume number.
- The last two digits indicate publication order within the volume using a Base 36 numbering system employing both numerals and letters. These two-number sets start with 00, 01, 02, 03, 04, 05, 06, 07, 08, 09, 0A, 0B ... 0Z, followed by 10-1Z, 20-2Z, etc.

The CID number appears on each page of the manuscript. The complete citation is used on the first page, and an abbreviated version on subsequent pages. Numbers in the index correspond to the last two digits of the six-digit CID number.

# Contents

## Part One

xvii *Conference Committee*  
xxi *Introduction*

---

### KEYNOTE SESSION

---

- 8353 02 **Advanced imaging research and development at DARPA (Keynote Paper)** [8353-29]  
N. K. Dhar, Defense Advanced Research Project Agency (United States); R. Dat, Booz Allen Hamilton (United States)

---

### NIR/SWIR FPAs AND APPLICATIONS

---

- 8353 03 **A high-resolution SWIR camera via compressed sensing** [8353-01]  
L. McMackin, M. A. Herman, B. Chatterjee, M. Weldon, InView Technology Corp. (United States)
- 8353 04 **Shortwave infrared camera with extended spectral sensitivity** [8353-02]  
M. Gerken, B. Achtner, M. Kraus, T. Neumann, M. Münzberg, Carl Zeiss Optronics GmbH (Germany)
- 8353 05 **SCD's cooled and uncooled photo detectors for NIR SWIR** [8353-03]  
R. Fraenkel, D. Aronov, Y. Benny, E. Berkowicz, L. Bykov, Z. Calahorra, T. Fishman, A. Giladi, E. Ilan, P. Klipstein, L. Langof, I. Lukomsky, Semiconductor Devices (Israel); D. Mistele, Technion (Israel); U. Mizrahi, D. Nussinson, Semiconductor Devices (Israel); A. Twitto, IMOD (Israel); M. Yassen, A. Zemel, Semiconductor Devices (Israel)
- 8353 06 **Flexible wide dynamic range VGA ROIC for InGaAs SWIR imaging** [8353-04]  
Y. Ni, B. Arion, Y. Zhu, B. Zongo, V. Noguier, P. Potet, New Imaging Technologies SAS (France)
- 8353 07 **High-performance 640 × 512 pixel hybrid InGaAs image sensor for night vision** [8353-05]  
E. De Borniol, F. Guellec, P. Castelein, CEA-LETI (France); A. Rouvié, J.-A. Robo, J.-L. Reverchon, Alcatel-Thales III-V Lab. (France)
- 8353 08 **InGaAs focal plane array developments at III-V Lab** [8353-06]  
A. Rouvié, J.-L. Reverchon, O. Huet, A. Djedidi, J.-A. Robo, J.-P. Truffer, T. Bria, M. Pires, J. Decobert, E. Costard, Alcatel-Thales III-V Lab. (France)
- 8353 09 **Low dark current small pixel large format InGaAs 2D photodetector array development at Teledyne Judson Technologies** [8353-07]  
H. Yuan, M. Meixell, J. Zhang, P. Bey, J. Kimchi, L. C. Kilmer, Teledyne Judson Technologies (United States)

- 8353 0A **Large-format InGaAs focal plane arrays for SWIR imaging** [8353-08]  
A. D. Hood, M. H. MacDougal, J. Manzo, D. Follman, J. C. Geske, FLIR Electro-Optical Components (United States)
- 8353 0B **A low-power, TEC-less, 1280 x 1024, compact SWIR camera with temperature-dependent, non-uniformity corrections** [8353-09]  
J. Nazemi, J. Battaglia, R. Brubaker, M. Delamere, C. Martin, Goodrich Corp. (United States)
- 8353 0C **Ultralow dark current CdHgTe FPAs in the SWIR range at CEA and SOFRADIR** [8353-10]  
O. Gravrand, L. Mollard, CEA-LETI (France); O. Boulade, V. Moreau, CEA-IRFU, Service d'Astrophysique (France); E. Sanson, SOFRADIR (France); G. Destefanis, CEA-LETI (France)
- 8353 0D **MT6425CA: a 640 x 512-25µm CTIA ROIC for SWIR InGaAs detector arrays** [8353-147]  
S. Eminoglu, Y. U. Mahsereci, C. Altiner, T. Akin, Mikro-Tasarim Ltd. (Turkey)

---

#### AIR FORCE INFRARED RESEARCH AND DEVELOPMENT

---

- 8353 0E **Multispectral imaging with type II superlattice detectors (Invited Paper)** [8353-11]  
G. Ariyawansa, J. M. Duran, M. Grupen, J. E. Scheihing, T. R. Nelson, M. T. Eismann, Air Force Research Lab. (United States)
- 8353 0F **Radiation tolerance of a dual-band IR detector based on a pBp architecture (Invited Paper)** [8353-141]  
V. M. Cowan, C. P. Morath, Air Force Research Lab. (United States); S. Myers, E. Plis, S. Krishna, Univ. of New Mexico (United States)
- 8353 0G **Space-based hyperspectral technologies for the thermal infrared (Invited Paper)** [8353-13]  
P. D. LeVan, Air Force Research Lab. (United States)
- 8353 0H **Hybrid dual-color MWIR detector for airborne missile warning systems (Invited Paper)** [8353-14]  
I. Hirsh, L. Shkedy, D. Chen, N. Fishler, Y. Hagbi, A. Koifman, Y. Openhaim, I. Vaserman, M. Singer, I. Shtrichman, Semiconductor Devices (SCD) (Israel)
- 8353 0I **Detection in urban scenario using combined airborne imaging sensors (Invited Paper)** [8353-15]  
I. Renhorn, M. Axelsson, Swedish Defence Research Agency (Sweden); K. Benoist, TNO Defence, Security and Safety (Netherlands); D. Bourghys, Royal Belgian Military Academy (Belgium); Y. Boucher, X. Briottet, ONERA (France); S. De Ceglie, CISAM (Italy); R. Dekker, TNO Defence, Security and Safety (Netherlands); A. Dimmeler, Fraunhofer-Institut für Optronik, Systemtechnik und Bildauswertung (Germany); R. Dost, National Aerospace Lab. NLR (Netherlands); O. Friman, Swedish Defence Research Agency (Sweden); I. Kåsen, Norwegian Defence Research Establishment (Norway); J. Maerker, Fraunhofer-Institut für Optronik, Systemtechnik und Bildauswertung (Germany); M. van Persie, National Aerospace Lab. NLR (Netherlands); S. Resta, CISAM (Italy); P. Schwering, TNO Defence, Security and Safety (Netherlands); M. Shimoni, Royal Belgian Military Academy (Belgium); T. V. Haavardsholm, Norwegian Defence Research Establishment (Norway)
- 8353 0J **Half-TV format MWIR sensor module incorporating proximity electronics (Invited Paper)** [8353-17]  
A. P. Ashcroft, L. Richardson, J. Harji, F. Giuliano, SELEX Galileo Infrared Ltd. (United Kingdom)

- 8353 OK **Comparison of the strapdown and gimbaled seekers utilized in aerial applications (Invited Paper)** [8353-18]  
B. Özkan, A. Uçar, TÜBİTAK SAGE (Turkey)
- 8353 OL **Anti-dazzling protection for Air Force pilots (Invited Paper)** [8353-19]  
A. Donval, T. Fisher, O. Lipman, M. Oron, KiloLambda Technologies, Ltd. (Israel)

---

#### THREAT ACQUISITION

---

- 8353 OM **Stereoscopic uncooled thermal imaging with autostereoscopic 3D flat-screen display in military driving enhancement systems** [8353-20]  
H. Haan, M. Münzberg, U. Schwarzkopf, Carl Zeiss Optronics GmbH (Germany);  
R. de la Barré, S. Jurk, B. Duckstein, Fraunhofer Heinrich Hertz Institute (Germany)
- 8353 ON **Infrared stereo camera for human machine interface** [8353-21]  
R. Edmondson, J. Vaden, D. Chenault, Polaris Sensor Technologies, Inc. (United States)
- 8353 OO **A compact deployable mid-wave infrared imaging system for wide-area persistence surveillance in maritime environments** [8353-23]  
K. P. Judd, Naval Research Lab. (United States); C. M. Colbert, R. Smith, Smart Logic, Inc. (United States); K. Vilardebo, V\_Systems, Inc. (United States); J. Waterman, Naval Research Lab. (United States); G. Petty, J. Kilzer, Naval Surface Warfare Ctr. (United States)
- 8353 OQ **Quantification of nitromethane with complementary super clip apodization and an iterative spectral comparison routine** [8353-25]  
K. J. Conroy, The Univ. of New South Wales (Australia); K. P. Kirkbride, Australian Federal Police (Australia); C. C. Harb, The Univ. of New South Wales (Australia)
- 8353 OR **On designing a SWIR multi-wavelength facial-based acquisition system** [8353-26]  
T. Bourlai, N. Narang, B. Cukic, L. Hornak, West Virginia Univ. (United States)
- 8353 OS **SWIR imaging for facial image capture through tinted materials** [8353-122]  
J. Ice, N. Narang, C. Whitelam, N. Kalka, L. Hornak, J. Dawson, T. Bourlai, West Virginia Univ. (United States)

---

#### TYPE II SUPERLATTICE FPAs I

---

- 8353 OT **Recent developments in type-II superlattice detectors at IRnova AB** [8353-27]  
H. Malm, R. M. von Würtemberg, C. Asplund, H. Martijn, IRnova AB (Sweden); A. Karim, Acreo AB (Sweden); O. Gustafsson, Royal Institute of Technology (Sweden); E. Plis, S. Krishna, Univ. of New Mexico (United States)
- 8353 OU **High-performance LWIR superlattice detectors and FPA based on CBIIRD design** [8353-28]  
A. Soibel, J. Nguyen, A. Khoshakhlagh, S. B. Rafol, L. Hoeglund, S. A. Keo, J. M. Mumolo, J. Liu, A. Liao, D. Z.-Y. Ting, S. D. Gunapala, Jet Propulsion Lab. (United States)
- 8353 OV **Development of type II superlattice detector for future space applications at JAXA** [8353-32]  
H. Katayama, J. Murooka, M. Naitoh, T. Imai, R. Sato, E. Tomita, M. Ueno, H. Murakami, Japan Aerospace Exploration Agency (Japan); S. Kawasaki, K. Bito, M. Kimata, Ritsumeikan Univ. (Japan); T. Kitada, T. Isu, Univ. of Tokushima (Japan); M. Patrashin, I. Hosako, National Institute of Information and Communications Technology (Japan)

---

**TYPE II SUPERLATTICE FPAs II**

---

- 8353 0W **1024 × 1024 LWIR SLS FPAs: status and characterization** [8353-35]  
M. Sundaram, A. Reisinger, R. Dennis, K. Patnaude, D. Burrows, J. Bundas, K. Beech, R. Faska, D. Manidakos, QmagiQ (United States)
- 8353 0X **Temperature-dependent absorption derivative on InAs/GaSb Type II superlattices** [8353-33]  
B. Klein, N. Gautam, S. Myers, S. Krishna, Univ. of New Mexico (United States)
- 8353 0Y **Electronic transport in InAs/GaSb type-II superlattices for long wavelength infrared focal plane array applications** [8353-34]  
G. A. Umana-Membreno, H. Kala, The Univ. of Western Australia (Australia); B. Klein, The Univ. of New Mexico (United States); J. Antoszewski, The Univ. of Western Australia (Australia); N. Gautam, M. N. Kuttly, E. Plis, S. Krishna, The Univ. of New Mexico (United States); L. Faraone, The Univ. of Western Australia (Australia)
- 8353 0Z **Passivation of type II InAs/GaSb superlattice photodetectors with atomic layer deposited Al<sub>2</sub>O<sub>3</sub>** [8353-36]  
O. Salihoglu, A. Muti, Bilkent Univ. (Turkey); K. Kutluer, T. Tansel, R. Turan, Middle East Technical Univ. (Turkey); C. Kocabas, A. Aydinli, Bilkent Univ. (Turkey)
- 8353 10 **Revolutionary development of Type-II GaSb/InAs superlattices for third generation of IR imaging (Invited Paper)** [8353-31]  
M. Razeghi, S. Abdollahi Pour, Northwestern Univ. (United States)
- 8353 11 **Analysis of surface oxides on narrow bandgap III-V semiconductors leading towards surface leakage free IR photodetectors** [8353-37]  
Q. Wang, X. Li, A. Zhang, S. Almqvist, A. Karim, B. Noharet, J. Y. Andersson, Acreo AB (Sweden); M. Göthelid, S. Yu, O. Gustafsson, M. Hammar, Royal Institute of Technology (Sweden); C. Asplund, IRnova AB (Sweden); E. Göthelid, Uppsala Univ. (Sweden)
- 8353 12 **Unrelaxed bulk InAsSb with novel absorption, carrier transport, and recombination properties for MWIR and LWIR photodetectors** [8353-38]  
D. Wang, Y. Lin, D. Donetsky, L. Shterengas, G. Kipshidze, G. Belenky, Stony Brook Univ. (United States); W. L. Sarney, H. Hier, S. P. Svensson, U.S. Army Research Lab. (United States)
- 8353 13 **100mm GaSb substrate manufacturing for IRFPA epi growth** [8353-39]  
L. P. Allen, J. P. Flint, G. Meshew, G. Dallas, J. Trevethan, Galaxy Compound Semiconductors, Inc. (United States); D. Lubyshev, Y. Qiu, J. M. Fastenau, A. W. K. Liu, IQE, Inc. (United States)
- 8353 14 **Large diameter 'ultra-flat' epitaxy ready GaSb substrates: requirements for MBE grown advanced infrared detectors** [8353-40]  
R. Martinez, S. Amirhaghi, B. Smith, A. Mowbray, M. J. Furlong, Wafer Technology Ltd. (United Kingdom)
- 8353 15 **Competing technology for high-speed HOT-IR-FPAs (Invited Paper)** [8353-91]  
M. Razeghi, S. A. Pour, Northwestern Univ. (United States)
- 8353 16 **Dark current modeling of MWIR type-II superlattice detectors** [8353-41]  
J. Wróbel, P. Martyniuk, Military Univ. of Technology (Poland); E. Plis, Univ. of New Mexico (United States); P. Madejczyk, W. Gawron, Military Univ. of Technology (Poland); S. Krishna, Univ. of New Mexico (United States); A. Rogalski, Military Univ. of Technology (Poland)

---

## EMERGING UNCOOLED TECHNOLOGIES

---

- 8353 17 **Uncooled silicon germanium oxide ( $\text{Si}_x\text{Ge}_y\text{O}_{1-x-y}$ ) thin films for infrared detection** [8353-105]  
M. L. Hai, M. Hesan, J. Lin, Q. Cheng, M. Jalal, Univ. of Missouri-Columbia (United States);  
A. J. Syllaios, S. Ajmera, L-3 Electro-Optical Systems (United States); M. Almasri, Univ. of  
Missouri-Columbia (United States)
- 8353 18 **Formation of GaN film on Si for microbolometer** [8353-43]  
Y. S. Lee, D.-S. Kim, C.-H. Won, J.-H. Kim, C.-H. Bu, S.-H. Hahm, Kyungpook National Univ.  
(Korea, Republic of); Y.-C. Jung, Kyeongju Univ. (Korea, Republic of); J.-H. Lee, Kyungpook  
National Univ. (Korea, Republic of)
- 8353 19 **Novel uncooled detector based on gallium nitride micromechanical resonators** [8353-44]  
V. J. Gokhale, Y. Sui, M. Rais-Zadeh, Univ. of Michigan (United States)
- 8353 1A **Nanobolometer: silicon-based uncooled multi-spectral IR detector** [8353-45]  
H. Lee, R. Verma, Tanner Research, Inc. (United States)
- 8353 1B **Development of microbolometer with high fill factor and high mechanical stability by  
shared-anchor structure** [8353-46]  
T. Kim, K. Kyung, J. H. Park, Y. S. Kim, S. K. Lim, K. Kim, K. Lee, National Nanofab Ctr. (Korea,  
Republic of); C. Welham, Coventor, SARL (France); H. Y. Kim, National Nanofab Ctr. (Korea,  
Republic of)
- 8353 1C **The first fabricated dual-band uncooled infrared microbolometer detector with a tunable  
micro-mirror structure** [8353-144]  
S. Keskin, T. Akin, Middle East Technical Univ. (Turkey)
- 8353 1D **An analysis for the broad-band absorption enhancement using plasmonic structures on  
uncooled infrared detector pixels** [8353-145]  
S. Z. Lulec, S. E. Kucuk, Middle East Technical Univ. (Turkey); E. Battal, A. K. Okyay, Bilkent Univ.  
(Turkey); M. Y. Tanrikulu, T. Akin, Middle East Technical Univ. (Turkey)

---

## UNCOOLED FPAs AND APPLICATIONS

---

- 8353 1E **An uncooled microbolometer focal plane array using heating-based resistance  
nonuniformity compensation** [8353-146]  
M. Tepegoz, A. Oguz, A. Toprak, S. U. Senveli, E. Canga, M. Y. Tanrikulu, T. Akin, Middle East  
Technical Univ. (Turkey)
- 8353 1F **Easy to use uncooled  $\frac{1}{4}$  VGA 17  $\mu\text{m}$  FPA development for high performance compact and  
low-power systems** [8353-49]  
P. Robert, J. Tissot, D. Pochic, V. Gravot, F. Bonnaire, H. Clerambault, A. Durand, S. Tinnes,  
ULIS (France)
- 8353 1G **Two-million-pixel SOI diode uncooled IRFPA with 15 $\mu\text{m}$  pixel pitch** [8353-50]  
D. Fujisawa, T. Maegawa, Y. Ohta, Y. Kosasayama, T. Ohnakado, H. Hata, M. Ueno, H. Ohji,  
Mitsubishi Electric Corp. (Japan); R. Sato, H. Katayama, T. Imai, M. Ueno, Japan Aerospace  
Exploration Agency (Japan)

- 8353 1H **Advanced  $\mu$ -bolometer detectors for high-end applications** [8353-51]  
U. Mizrahi, F. Schapiro, L. Bykov, A. Giladi, N. Shiloah, I. Pivnik, S. Elkind, S. Maayani  
E. Mordechai, O. Farbman, Y. Hirsh, Semiconductor Devices (SCD) (Israel); A. Twitto,  
M. Ben-Ezra, Israeli MOD (Israel); A. Fraenkel, Semiconductor Devices (SCD) (Israel)
- 8353 1I **Current progress on pixel level packaging for uncooled IRFPA** [8353-52]  
G. Dumont, W. Rabaud, J.-J. Yon, L. Carle, V. Goudon, C. Vialle, S. Becker, A. Hamelin,  
A. Arnaud, CEA-LETI, MINATEC (France)
- 8353 1J **The estimation of thermal properties of  $\mu$ -bolometers in a FPA with some selected structures and pitches** [8353-128]  
S. Park, S. Han, C. S. Han, Hoseo Univ. (Korea, Republic of); H. C. Lee, KAIST (Korea, Republic of)
- 8353 1K **Parylene supported 20 $\mu$ m\*20 $\mu$ m uncooled thermoelectric infrared detector with high fill factor** [8353-131]  
M. J. Modarres-Zadeh, Z. S. Carpenter, M. G. Rockley, R. Abdolvand, Oklahoma State Univ. (United States)
- 8353 1L **New high detectivity linear array for analytical measurement in the room temperature range** [8353-110]  
F. Haenschke, E. Kessler, U. Dillner, A. Ihring, U. Schinkel, H.-G. Meyer, Institute of Photonic Technology (Germany)

---

**SMART PROCESSING: JOINT SESSION WITH CONFERENCE 8355**

- 8353 1M **An information-theoretic perspective on the challenges and advances in the race toward 12 $\mu$ m pixel pitch megapixel uncooled infrared imaging** [8353-53]  
C.-L. Tisse, MTech-Imaging Pte. Ltd. (Singapore); J.-L. Tissot, A. Crastes, ULIS (France)
- 8353 1N **Flexible readout and integration sensor (FRIS): a bio-inspired, system-on-chip, event-based readout architecture** [8353-54]  
J. H. Lin, P. O. Pouliquen, A. G. Andreou, The Johns Hopkins Univ. (United States);  
A. C. Goldberg, C. G. Rizk, The Johns Hopkins Univ. Applied Physics Lab. (United States)
- 8353 1O **ADMIRE: a locally adaptive single-image, non-uniformity correction and denoising algorithm: application to uncooled IR camera** [8353-55]  
Y. Tendo, École Normale Supérieure de Cachan (France); J. Gilles, Univ. of California, Los Angeles (United States)
- 8353 1P **Commercially developed mixed-signal CMOS process features for application in advanced ROICs in 0.18 $\mu$ m technology node** [8353-127]  
A. Kar-Roy, P. Hurwitz, R. Mann, Y. Qamar, S. Chaudhry, R. Zwingman, D. Howard,  
M. Racanelli, TowerJazz (United States)
- 8353 1Q **Design and realization of 144  $\times$  7 TDI ROIC with hybrid integrated test structure** [8353-129]  
O. Ceylan, H. Kayahan, M. Yazici, M. B. Baran, Y. Gurbuz, Sabanci Univ. (Turkey)

## Part Two

---

### CRYOCOOLERS FOR IR FOCAL PLANE ARRAYS

---

- 8353 1R **Thales Cryogenics rotary cryocoolers for HOT applications** [8353-56]  
J.-Y. Martin, J.-M. Cauquil, Thales Cryogénie S.A.S. (France); T. Benschop, Thales Cryogenics B.V. (Netherlands); S. Freche, Thales Cryogénie S.A.S. (France)
- 8353 1S **Update on MTF figures for linear and rotary coolers of Thales Cryogenics** [8353-57]  
W. van de Groep, H. van der Weijden, R. van Leeuwen, T. Benschop, Thales Cryogenics B.V. (Netherlands); J. M. Cauquil, R. Griot, Thales Cryogénie S.A.S. (France)
- 8353 1T **Compact high-efficiency linear cryocooler in single-piston moving magnet design for HOT detectors** [8353-58]  
I. Rühlich, M. Mai, C. Rosenhagen, A. Withopf, S. Zehner, AIM INFRAROT-MODULE GmbH (Germany)
- 8353 1U **RICOR's rotary cryocoolers development and optimization for HOT IR detectors** [8353-59]  
A. Filis, Z. Bar Haim, T. Havatzelet, D. Gover, M. Barak, RICOR-Cryogenic & Vacuum Systems (Israel)
- 8353 1V **Linear cryogenic coolers for HOT infrared detectors** [8353-60]  
A. Veprik, S. Riabzev, RICOR-Cryogenic & Vacuum Systems (Israel); N. Avishay, Elbit Systems, Electro-Optics - ELOP (Israel); D. Oster, A. Tuitto, Israel Ministry of Defense (Israel)
- 8353 1W **Experimental demonstration of cryocooler electronics with multiple mechanical cryocooler types** [8353-61]  
J. J. Freeman, J. B. Murphy, C. S. Kirkconnell, Iris Technology Corp. (United States)

---

### IR OPTICS I

---

- 8353 1X **Common aperture multispectral optics for military applications** [8353-62]  
N. A. Thompson, Qioptiq Ltd. (United Kingdom)
- 8353 1Y **Multi-field of view see-spot optics** [8353-66]  
S. Lilley, J. Vizgaitis, U.S. Army Night Vision & Electronic Sensors Directorate (United States); J. Everett, B. Spinazzola, General Dynamics-Global Imaging Technologies (United States)
- 8353 1Z **Single layer spectro-polarimetric filter for advanced LWIR FPAs** [8353-64]  
A. M. Jones, Sandia National Labs. (United States) and The Univ. of Arizona (United States); S. A. Kemme, D. A. Scrymgeour, Sandia National Labs. (United States); R. A. Norwood, The Univ. of Arizona (United States)
- 8353 20 **Low reflectance DLC coatings on various IR substrates** [8353-65]  
M. Gilo, A. Azran, Ophir Optonics Ltd. (Israel)

## IR OPTICS II

---

- 8353 21 **Planar integrated plasmonic mid-IR spectrometer** [8353-63]  
C. J. Fredricksen, LRC Engineering, Inc. (United States); J. W. Cleary, Air Force Research Lab. (United States); W. R. Buchwald, Solid State Scientific Corp. (United States); P. Figueiredo, F. Khalilzadeh-Rezaie, G. Medhi, I. Rezadad, M. Shahzad, M. Yesiltas, J. Nath, J. Boroumand, E. Smith, R. E. Peale, Univ. of Central Florida (United States)
- 8353 22 **Integration of wide field-of-view imagery functions in a detector dewar cooler assembly** [8353-67]  
G. Druart, F. de la Barriere, N. Guerineau, ONERA (France); G. Lasfargues, M. Fendler, N. Lhermet, CEA-LETI, MINATEC (France); J. Taboury, Institut d'Optique Graduate School (France); Y. Reibel, SOFRADIR (France); J.-B. Moullec, Direction Générale de L'armement (France)
- 8353 23 **Infrared focal plane array with a built-in stationary Fourier-transform spectrometer: recent technological advances** [8353-68]  
Y. Ferrec, N. Guérineau, S. Rommeluère, S. Lefebvre, F. de la Barrière, ONERA (France); G. Lasfargues, M. Fendler, CEA-LETI, MINATEC (France)
- 8353 24 **Laser designator protection filter for see-spot thermal imaging systems** [8353-70]  
A. Donval, T. Fisher, O. Lipman, M. Oron, KiloLambda Technologies, Ltd. (Israel)
- 8353 25 **Passive athermalization of two-lens designs in 8-12micron waveband** [8353-71]  
N. Schuster, Umicore Electro-Optic Materials (Belgium); J. Franks, Umicore Coating Services (United Kingdom)
- 8353 26 **Advantages of using engineered chalcogenide glass for color corrected, passively athermalized LWIR imaging systems** [8353-72]  
K. Schwertz, A. Bublitz, S. Sparrold, Edmund Optics Inc. (United States)
- 8353 27 **Qualification and metrology for US-produced chalcogenides** [8353-73]  
N. Carlie, SCHOTT North America, Inc. (United States)
- 8353 28 **Material trades between Be, SiC, and VQ aluminum for tactical systems: update referencing the current state-of-the-art** [8353-74]  
C. J. Duston, T. Hull, L-3 Integrated Optical Systems (United States)
- 8353 29 **Mid-spatial frequency matters: examples of the control of the power spectral density and what that means to the performance of imaging systems** [8353-75]  
T. Hull, L-3 Integrated Optical Systems Division (United States) and The Univ. of New Mexico (United States); M. J. Riso, J. M. Barentine, A. Magruder, L-3 Integrated Optical Systems Division (United States)
- 8353 2A **Advances in shutter drive technology to enhance man-portable infrared cameras** [8353-142]  
D. Durfee, CVI Melles Griot (United States)
- 8353 2B **Study on optimizing the thickness of silicon window of WLP for IR sensor** [8353-121]  
M. Song, National Nanofab Ctr. (Korea, Republic of) and Chungnam National Univ. (Korea, Republic of); T. H. Kim, M. S. Hyun, J. H. Park, H. Y. Kim, National Nanofab Ctr. (Korea, Republic of); G. Lee, Chungnam National Univ. (Korea, Republic of)

8353 2C **Update on Tinsley visible quality (VQ) aluminum optics** [8353-132]  
A. M. Patel, K. G. Carrigan, L-3 Integrated Optical Systems Div. (United States)

8353 2D **Manufacturing status of Tinsley visible quality bare aluminum and an example of snap together assembly** [8353-133]  
K. G. Carrigan, L-3 Integrated Optical Systems (United States)

---

#### ACTIVE IMAGING

---

8353 2E **16 channel GHz low noise SWIR photoreceivers** [8353-76]  
X. Bai, P. Yuan, P. McDonald, J. Boisvert, J. Chang, R. Woo, E. Labios, R. Sudharsanan, Boeing Spectrolab Inc. (United States); M. Krainak, G. Yang, X. Sun, W. Lu, NASA Goddard Space Flight Ctr. (United States); D. McIntosh, Q. Zhou, J. Campbell, Univ. of Virginia (United States)

8353 2F **Advances in Ladar components and subsystems at Raytheon** [8353-77]  
M. Jack, G. Chapman J. Edwards, W. Mc Keag, T. Veeder, J. Wehner, Raytheon Vision Systems (United States); T. Roberts, T. Robinson, J. Neisz, C. Andressen, R. Rinker, Ratheown Missile Systems (United States); D. N. B. Hall, S. M. Jacobson, Univ. of Hawai'i (United States); F. Amzajerdian, NASA Langley Research Ctr. (United States); T. D. Cook, Naval Air Warfare Ctr. (United States)

8353 2G **Small pixel pitch solutions for active and passive imaging** [8353-78]  
Y. Reibel, A. Kerlain, G. Bonnouvier, D. Billon-Lanfrey, SOFRADIR (France); J. Rothman, L. Mollard, E. de Borniol, G. Destefanis, CEA-LETI, MINATEC (France)

8353 2H **Development of low excess noise SWIR APDs** [8353-79]  
X. Bai, P. Yuan, P. McDonald, J. Boisvert, J. Chang, R. Sudharsanan, Boeing Spectrolab Inc. (United States); M. Krainak, G. Yang, X. Sun, W. Lu, NASA Goddard Space Flight Ctr. (United States); Z. Lu, Q. Zhou, W. Sun, J. Campbell, Univ. of Virginia (United States)

---

#### HGCDTE I

---

8353 2I **Mercury cadmium telluride (HgCdTe) passivation by advanced thin conformal Al<sub>2</sub>O<sub>3</sub> films** [8353-80]  
R. Fu, J. Pattison, A. Chen, O. Nayfeh, U.S. Army Research Lab. (United States)

8353 2J **12µm pixel pitch development for 3-side butttable megapixel MW FPAs** [8353-81]  
P. Thorne, H. Weller, L. G. Hipwood, SELEX Galileo Infrared Ltd. (United Kingdom)

8353 2K **Status of MCT focal plane arrays in France** [8353-82]  
M. Vuillermet, D. Billon-Lanfrey, Y. Reibel, A. Manissadjian, SOFRADIR (France); L. Mollard, N. Baier, O. Gravranc, G. Destéfanis, CEA-LETI, MINATEC (France)

8353 2L **State-of-the-art MCT IR-modules with enhanced long term and cycle stability** [8353-83]  
R. Breiter, J. Wendler, H. Lutz, S. Rutzinger, T. Schallenberg, J. Ziegler, I. Rühlich, AIM INFRAROT-MODULE GmbH (Germany)

8353 2M **SWIR and NIR MCT arrays grown by MOVPE for astronomy applications** [8353-84]  
L. G. Hipwood, N. Shorrocks, C. Maxey, SELEX Galileo Infrared Ltd. (United Kingdom); D. Atkinson, N. Bezawada, UK Astronomy Technology Ctr. (United Kingdom)

- 8353 2N **Very long wavelength infrared detection with p-on-n LPE HgCdTe** [8353-85]  
N. Baier, L. Mollard, O. Gravrand, G. Bourgeois, J.-P. Zanatta, G. Destefanis, CEA-LETI, MINATEC (France); P. Pidancier, P. Chorier, SOFRADIR (France); L. Tauziède, A. Bardoux, Ctr. National d'Etudes Spatiales (France)
- 8353 2O **LWIR and VLWIR MCT technologies and detectors development at SOFRADIR for space applications** [8353-115]  
C. Leroy, P. Chorier, SOFRADIR (France); G. Destefanis, CEA-LETI, MINATEC (France)

---

#### HGCDTE II

---

- 8353 2P **Electrical characteristics of MOVPE grown MWIR N<sup>+</sup>p(As)HgCdTe heterostructure photodiodes build on GaAs substrates** [8353-86]  
R. E. DeWames, J. G. Pellegrino, U.S. Army Night Vision & Electronic Sensors Directorate (United States)
- 8353 2Q **State of MBE technology at AIM** [8353-87]  
J. Wenisch, D. Eich, H. Lutz, T. Schallenberg, R. Wollrab, J. Ziegler, AIM INFRAROT-MODULE GmbH (Germany)
- 8353 2R **High operating temperature mid-wavelength infrared HgCdTe photon trapping focal plane arrays** [8353-88]  
K. D. Smith, J. G. A. Wehner, R. W. Graham, J. E. Randolph, A. M. Ramirez, G. M. Venzor, K. Olsson, M. F. Vilela, E. P. G. Smith, Raytheon Vision Systems (United States)
- 8353 2S **Laser power and temperature dependence on laser beam induced current signal in As-doped p-type HgCdTe** [8353-137]  
Y. Chen, W. Hu, X. Chen, Z. Ye, J. Wang, C. Lin, X. Hu, W. Lu, Shanghai Institute of Technical Physics (China)
- 8353 2T **Studies on a novel mask technique with high selectivity and aspect-ratio patterns for HgCdTe trenches ICP etching** [8353-119]  
Z. H. Ye, W. D. Hu, Shanghai Institute of Technical Physics (China); Y. Li, J. Huang, W. T. Yin, Shanghai Institute of Technical Physics (China) and Graduate School of the Chinese Academy of Sciences (China); C. Lin, X. N. Hu, R. J. Ding, X. S. Chen, W. Lu, L. He, Shanghai Institute of Technical Physics (China)
- 8353 2U **Infrared detection module for optoelectronic sensors** [8353-125]  
W. Gawron, Z. Bielecki, J. Wojtas, Military Univ. of Technology (Poland); D. Stanaszek, J. Łach, M. Fimiarz, VIGO Systems S.A. (Poland)
- 8353 2V **Application of advanced IR-FPA in high-sensitivity pushbroom SWIR hyperspectral imager** [8353-139]  
Y. Wang, X. Zhuang, S. Wang, J. Wang, Shanghai Institute of Technical Physics (China)

---

#### HOT: HIGH-OPERATING TEMPERATURE FPAs

---

- 8353 2W **MWIR mercury cadmium telluride detectors for high operating temperatures (Invited Paper)** [8353-89]  
L. Pillans, R. M. Ash, L. Hipwood, P. Knowles, SELEX Galileo Infrared Ltd. (United Kingdom)

- 8353 2X **HOT MWIR HgCdTe performance on CZT and alternative substrates (Invited Paper)** [8353-90]  
J. G. Pellegrino, R. DeWames, P. Perconti, C. Billman, P. Maloney, U.S. Army Night Vision & Electronic Sensors Directorate (United States)
- 8353 2Y **High operating temperature epi-InSb and X<sub>Bn</sub>-InAsSb photodetectors (Invited Paper)** [8353-92]  
I. Shtrichman, D. Aronov, Semiconductor Devices (SCD) (Israel); M. ben Ezra, Israel MOD (Israel); I. Barkai, E. Berkowicz, M. Brumer, R. Fraenkel, A. Glzman, S. Grossman, E. Jacobsohn, O. Klin, P. Klipstein, I. Lukomsky, L. Shkedy, N. Snapi, M. Yassen, E. Weiss, Semiconductor Devices (SCD) (Israel)
- 8353 2Z **Photoconductive gain in barrier heterostructure infrared detectors** [8353-93]  
S. Myers, B. Klein, E. Plis, N. Gautam, Univ. of New Mexico (United States); C. Morath, V. Cowan, Air Force Research Lab. (United States); S. Krishna, Univ. of New Mexico (United States)
- 8353 30 **Numerical simulation of InAs/AlAsSb nBn detector arrays** [8353-94]  
J. Schuster, B. Pinkie, Boston Univ. (United States); M. Reine, Consultant (United States); E. Bellotti, Boston Univ. (United States)
- 8353 31 **320 × 256 complementary barrier infrared detector focal plane array for long-wave infrared imaging** [8353-95]  
J. Nguyen, S. B. Rafol, A. Soibel, A. Khoskhlagh, D. Z.-Y. Ting, J. K. Liu, J. M. Mumolo, S. D. Gunapala, Jet Propulsion Lab. (United States)
- 8353 32 **High operating temperature midwave quantum dot barrier infrared detector (QD-BIRD)** [8353-96]  
D. Z. Ting, A. Soibel, C. J. Hill, S. A. Keo, J. M. Mumolo, S. D. Gunapala, Jet Propulsion Lab. (United States)
- 8353 33 **MWIR InAs<sub>1-x</sub>Sb<sub>x</sub> nCBn detectors data and analysis** [8353-97]  
A. I. D'Souza, E. Robinson, A. C. Ionescu, D. Okertund, DRS Sensors & Targeting Systems, Inc. (United States); T. J. de Lyon, R. D. Rajavel, H. Sharifi, D. Yap, HRL Labs., LLC (United States); N. Dhar, Defense Advanced Research Projects Agency (United States); P. S. Wijewarnasuriya, U.S. Army Research Lab. (United States); C. Grein, Univ. of Illinois at Chicago (United States)
- 8353 34 **Improved IR detectors to swap heavy systems for SWaP** [8353-98]  
A. Manissadjian, L. Rubaldo, Y. Rebeil, A. Kerlain, SOFRADIR (France); D. Brellier, L. Mollard, CEA-LETI, MINATEC (France)
- 8353 35 **Modeling of dark current suppression in unipolar barrier infrared detectors** [8353-138]  
J. Wang, Shanghai Institute of Technical Physics (China) and Univ. of Science and Technology of China (China); X. Chen, W. Hu, Y. Chen, L. Wang, W. Lu, Shanghai Institute of Technical Physics (China); F. Xu, Univ. of Science and Technology of China (China)

---

## QWIP AND Q-DOT

---

- 8353 36 **Sub-monolayer InAs/InGaAs quantum dot infrared photodetectors (SML-QDIP)** [8353-99]  
J. O. Kim, S. Sengupta, Y. Sharma, A. V. Barve, Univ. of New Mexico (United States); S. J. Lee, S. K. Noh, Korean Research Institute of Standards and Science (Korea, Republic of); S. Krishna, Univ. of New Mexico (United States)
- 8353 37 **Solution-processed colloidal quantum dot photodiodes for low-cost SWIR imaging** [8353-100]  
E. J. D. Klem, J. Lewis, C. Gregory, G. Cunningham, D. Temple, RTI International (United States)
- 8353 38 **Demonstration of high responsivity (~2.16 A/W) and detectivity (~10<sup>11</sup> Jones) in the long wavelength (~10.2 μm) from InGaAs/GaAs quantum dot infrared photodetector with quaternary InAlGaAs capping** [8353-101]  
S. Chakrabarti, S. Adhikary, N. Halder, Indian Institute of Technology Bombay (India); Y. Aytac, A. G. U. Perera, Georgia State Univ. (United States)
- 8353 39 **QWIP infrared detector production line results** [8353-102]  
M. Runtz, F. Perrier, N. Ricard, SOFRADIR (France); E. Costard, A. Nedelcu, Alcatel-Thales III-V Lab. (France); V. Guériaux, Alcatel-Thales III-V Lab. (France) and Thales Optronique S.A. (France)

---

## SELECTED DETECTOR TECHNOLOGIES

---

- 8353 3A **Design and development of carbon nanotube-based microbolometer for IR imaging applications** [8353-103]  
A. K. Sood, E. J. Egerton, Y. R. Puri, Magnolia Optical Technologies, Inc. (United States); G. Fernandes, J. Xu, Brown Univ. (United States); A. Akturk, N. Goldsman, Cool CAD Electronics, LLC (United States); N. K. Dhar, Defense Advanced Research Projects Agency/MTO (United States); M. Dubey, P. S. Wijewarnasuriya, U.S. Army Research Lab. (United States); B. I. Lineberry, Defense Advanced Research Projects Agency (United States)
- 8353 3B **Nanoantenna-enabled midwave infrared focal plane arrays** [8353-104]  
D. W. Peters, C. M. Reinke, P. S. Davids, J. F. Klem, D. Leonhardt, J. R. Wendt, J. K. Kim, S. Samora, Sandia National Labs. (United States)
- 8353 3C **Lifetime prediction in vacuum packaged MEMS provided with integrated getter film** [8353-106]  
F. Siviero, A. Bonucci, A. Conte, M. Moraja, SAES Getters S.p.A. (Italy); O. Gigan, TRONICS Microsystems (France); I. Thomas, Thales Avionics S.A. (France)
- 8353 3D **High-speed, large-area, p-i-n InGaAs photodiode linear array at 2-micron wavelength** [8353-107]  
A. Joshi, S. Datta, Discovery Semiconductors, Inc. (United States)
- 8353 3E **NIR/LWIR dual-band infrared photodetector with optical addressing** [8353-109]  
O. O. Cellek, H. S. Kim, Arizona State Univ. (United States); J. L. Reno, Sandia National Labs. (United States); Y.-H. Zhang, Arizona State Univ. (United States)

- 8353 3F **InAs/InAsSb Type-II superlattice: a promising material for mid-wavelength and long-wavelength infrared applications** [8353-136]  
O. O. Cellek, H. Li, X.-M. Shen, Z. Lin, E. H. Steenbergen, D. Ding, S. Liu, Q. Zhang, H. S. Kim, J. Fan, M. J. DiNezza, W. H. G. Dettlaff, P. T. Webster, Z. He, J.-J. Li, S. R. Johnson, D. J. Smith, Y.-H. Zhang, Arizona State Univ. (United States)
- 8353 3G **Initial testing of a Si:As blocked-impurity-band (BIB) trap detector** [8353-126]  
S. I. Woods, S. G. Kaplan, National Institute of Standards and Technology (United States); T. M. Jung, Jung Research and Development Corp. (United States); A. C. Carter, Booz Allen Hamilton Inc. (United States); J. E. Proctor, Joptech Inc. (United States)

---

#### VARIOUS APPLICATIONS OF SELECTED DETECTOR TECHNOLOGIES

---

- 8353 3H **IR CMOS: ultrafast laser-enhanced silicon imaging** [8353-111]  
M. U. Pralle, J. E. Carey, H. Homayoon, J. Sickler, X. Li, J. Jiang, C. Hong, F. Sahebi, C. Palsule, J. McKee, SiOnyx Inc. (United States)
- 8353 3I **Location precision analysis of stereo thermal anti-sniper detection system** [8353-140]  
Y. He, Y. Lu, X. Zhang, W. Jin, Beijing Institute of Technology (China)
- 8353 3J **Development of the Compact Infrared Camera (CIRC) for earth observation** [8353-114]  
E. Kato, H. Katayama, M. Naitoh, M. Harada, R. Nakamura, R. Sato, Japan Aerospace Exploration Agency (Japan)

*Author Index*



## Conference Committee

### *Symposium Chair*

**Kevin P. Meiners**, Office of the Secretary of Defense (United States)

### *Symposium Cochair*

**Kenneth R. Israel**, Lockheed Martin Corporation (United States)

### *Conference Chairs*

**Bjørn F. Andresen**, Israel Aerospace Industries Ltd. (Israel)

**Gabor F. Fulop**, Maxtech International, Inc. (United States)

**Paul R. Norton**, U.S. Army Night Vision & Electronic Sensors Directorate  
(United States)

### *Program Committee*

**Christopher C. Alexay**, StingRay Optics, LLC (United States)

**Jagmohan Bajaj**, Teledyne Imaging Sensors (United States)

**Stefan T. Baur**, Raytheon Company (United States)

**Philippe F. Bois**, Alcatel-Thales III-V Lab (France)

**Wolfgang A. Cabanski**, AIM INFRAROT-MODULE GmbH (Germany)

**John T. Caulfield**, Cyan Systems (United States)

**John W. Devitt**, Georgia Tech Research Institute (United States)

**Nibir K. Dhar**, Defense Advanced Research Projects Agency (United  
States)

**Michael T. Eismann**, Air Force Research Laboratory (United States)

**Mark E. Greiner**, L-3 Communications Cincinnati Electronics  
(United States)

**Sarath D. Gunapala**, Jet Propulsion Laboratory (United States)

**Charles M. Hanson**, L-3 Electro-Optical Systems (United States)

**Masafumi Kimata**, Ritsumeikan University (Japan)

**Hee Chul Lee**, KAIST (Korea, Republic of)

**Paul D. LeVan**, Air Force Research Laboratory (United States)

**Chuan C. Li**, DRS Technologies, Inc. (United States)

**Wei Lu**, Shanghai Institute of Technical Physics (China)

**Michael H. MacDougall**, FLIR Electro-Optical Components (United  
States)

**Tara J. Martin**, Sensors Unlimited, Inc., part of Goodrich Corporation  
(United States)

**Paul L. McCarley**, Air Force Research Laboratory (United States)

**R. Kennedy McEwen**, SELEX Galileo Infrared Ltd. (United Kingdom)

**John L. Miller**, FLIR Systems, Inc. (United States)

**A. Fenner Milton**, U.S. Army Night Vision & Electronic Sensors Directorate  
(United States)

**Mario O. Münzberg**, Carl Zeiss Optronics GmbH (Germany)

**Peter W. Norton**, BAE Systems (United States)

**Bob Owen**, L-3 Communications Infrared Products (United States)

**Joseph G. Pellegrino**, U.S. Army Night Vision & Electronic Sensors  
Directorate (United States)

**Ray Radebaugh**, National Institute of Standards and Technology  
(United States)

**Manijeh Razeghi**, Northwestern University (United States)

**Colin E. Reese**, U.S. Army Night Vision & Electronic Sensors Directorate  
(United States)

**Ingmar G. Renhorn**, Swedish Defence Research Agency (Sweden)

**Antoni Rogalski**, Military University of Technology (Poland)

**Ingo Rühlich**, AIM INFRAROT-MODULE GmbH (Germany)

**Piet B. W. Schwing**, TNO Defence, Security and Safety (Netherlands)

**Itay Shtrichman**, SCD Semiconductor Devices (Israel)

**Rengarajan Sudharsanan**, Spectrolab, Inc. (United States)

**Stefan P. Svensson**, U.S. Army Research Laboratory (United States)

**Venkataraman S. Swaminathan**, U.S. Army Armament Research,  
Development and Engineering Center (United States)

**Simon Thibault**, University Laval (Canada)

**Gil A. Tidhar**, Optigo Directorate IAI-Elta (Israel)

**Meimei Z. Tidrow**, U.S. Army Night Vision & Electronic Sensors  
Directorate (United States)

**Jean-Luc M. Tissot**, ULIS (France)

**Alexander Vepruk**, RICOR-Cryogenic & Vacuum Systems (Israel)

**Jay N. Vizgaitis**, U.S. Army Night Vision & Electronic Sensors Directorate  
(United States)

**Michel Vuillermet**, SOFRADIR (France)

**James R. Waterman**, U.S. Naval Research Laboratory (United States)

**Lucy Zheng**, Institute for Defense Analyses (United States)

#### *Session Chairs*

- 1 NIR/SWIR FPAs and Applications  
**Tara J. Martin**, Sensors Unlimited, Inc., part of Goodrich Corporation  
(United States)  
**Michael H. MacDougall**, FLIR Electro-Optical Components  
(United States)
- 2 Air Force Infrared Research and Development  
**Paul D. LeVan**, Air Force Research Laboratory (United States)  
**R. Kennedy McEwen**, SELEX Galileo (United Kingdom)

- 3 Threat Acquisition  
**Mario O. Münzberg**, Carl Zeiss Optronics GmbH (Germany)  
**Gil A. Tidhar**, IAI-Elta Systems Ltd. (Israel)
  
- 4 Type II Superlattice FPAs I  
**Meimei Z. Tidrow**, U.S. Army Night Vision & Electronic Sensors Directorate (United States)  
**Manijeh Razeghi**, Northwestern University (United States)  
**Lucy Zheng**, Institute for Defense Analyses (United States)
  
- 5 Keynote Session  
**Bob Owen**, L-3 Communications Infrared Products (United States)
  
- 6 Type II Superlattice FPAs II  
**Meimei Z. Tidrow**, U.S. Army Night Vision & Electronic Sensors Directorate (United States)  
**Manijeh Razeghi**, Northwestern University (United States)  
**Lucy Zheng**, Institute for Defense Analyses (United States)
  
- 7 Emerging Uncooled Technologies  
**Colin E. Reese**, U.S. Army Night Vision & Electronic Sensors Directorate (United States)  
**Charles M. Hanson**, Consultant in Infrared (United States)
  
- 8 Uncooled FPAs and Applications  
**Jean-Luc M. Tissot**, ULIS (France)  
**Masafumi Kimata**, Ritsumeikan University (Japan)  
**Avraham Fraenkel**, SCD Semiconductor Devices (Israel)
  
- 9 Smart Processing: Joint Session with Conference 8355  
**Richard L. Espinola**, U.S. Army Night Vision & Electronic Sensors Directorate (United States)  
**Endre Repasi**, Fraunhofer-Institut für Optronik, Systemtechnik und Bildauswertung (Germany)  
**Paul L. McCarley**, Air Force Research Laboratory (United States)  
**Bob Owen**, L-3 Communications Infrared Products (United States)
  
- 10 Cryocoolers for IR Focal Plane Arrays  
**Alexander Veprik**, RICOR-Cryogenic & Vacuum Systems (Israel)  
**Ingo Rühlich**, AIM INFRAROT-MODULE GmbH (Germany)  
**Ray Radebaugh**, National Institute of Standards and Technology (United States)
  
- 11 IR Optics I  
**Christopher C. Alexay**, StingRay Optics, LLC (United States)  
**Jay N. Vizgaitis**, U.S. Army Night Vision & Electronic Sensors Directorate (United States)

- 12 IR Optics II  
**Christopher C. Alexay**, StingRay Optics, LLC (United States)  
**Jay N. Vizgaitis**, U.S. Army Night Vision & Electronic Sensors Directorate  
(United States)
- 13 Active Imaging  
**Stefan T. Baur**, Raytheon Company (United States)  
**Ingmar G. Renhorn**, Swedish Defence Research Agency (Sweden)
- 14 HgCdTe I  
**Joseph G. Pellegrino**, U.S. Army Night Vision & Electronic Sensors  
Directorate (United States)  
**Michel Vuillermet**, SOFRADIR (France)
- 15 HgCdTe II  
**Michel Vuillermet**, SOFRADIR (France)  
**Joseph G. Pellegrino**, U.S. Army Night Vision & Electronic Sensors  
Directorate (United States)
- 16 HOT: High-Operating Temperature FPAs  
**Michael T. Eismann**, Air Force Research Laboratory (United States)  
**Stuart B. Horn**, U.S. Army Night Vision & Electronic Sensors Directorate  
(United States)
- 17 QWIP and Q-DOT  
**Eric M. Costard**, Alcatel-Thales III-V Lab (France)
- 18 Selected Detector Technologies  
**John W. Devitt**, Georgia Tech Research Institute (United States)
- 19 Various Applications of Selected Detector Technologies  
**Bjørn F. Andresen**, Israel Aerospace Industries Ltd. (Israel)  
**Paul R. Norton**, U.S. Army Night Vision & Electronic Sensors Directorate  
(United States)

# Introduction

The Thirty-Eighth conference on Infrared Technology and Applications was held the week of April 23-27, 2012 at the Baltimore Convention Center in Baltimore, Maryland. The agenda was divided into 19 sessions:

1. NIR/SWIR FPAs and Applications
2. Air Force Infrared Research and Development
3. Threat Acquisition
4. Type II Superlattice FPAs I
5. Keynote Session—  
Advanced imaging R&D at DARPA-MTO
6. Type II Superlattice FPAs II
7. Emerging Uncooled Technologies
8. Uncooled FPAs and Applications
9. Smart Processing
10. Cryocoolers for IR Focal Plane Arrays
11. IR Optics I
12. IR Optics II
13. Active Imaging
14. HgCdTe I
15. HgCdTe II
16. HOT—High Operating Temperature FPAs
17. QWIP and QDOT
18. Selected Detector Technologies
19. Various Applications of Selected Detector Technologies

In addition, there were twenty-one poster papers presented for discussion on Thursday evening—these have been added to the 19 sessions in the Proceedings. Highlights of six topical areas that are summarized below:

- Keynote
- Photon detectors
- Uncooled detectors
- Optics
- Cryocoolers
- Smart image and signal processing
- Applications

## Keynote

The Keynote address reviewed five key programs at DARPA MTO in infrared imaging:

- Very wide field-of-view infrared sensors—in a 10 Giga-pixel architecture.
- Small pitch FPAs— $5\ \mu\text{m}$  for the LWIR—see Fig. 1.
- Broadband and HOT FPAs—using photon trapping arrays on HgCdTe or InAsSb nBn FPAs—see Fig. 2.
- Multiband and tunable FPAs—integrated vis/NIR/SWIR and LWIR—see Fig. 3.
- Very low cost uncooled FPAs—wafer-level-packaged, ultra-low cost small pixel microbolometers, integrated electronics and molded optics.
- Networked uncooled FPAs— $1280\times 1024$  and  $640\times 480$ —for soldier situational awareness—using an Android PDA.

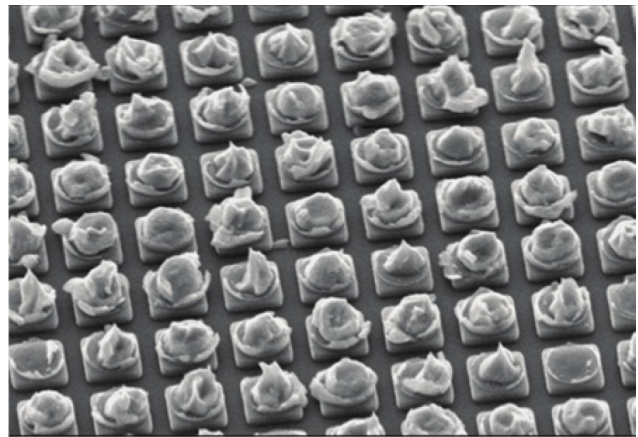
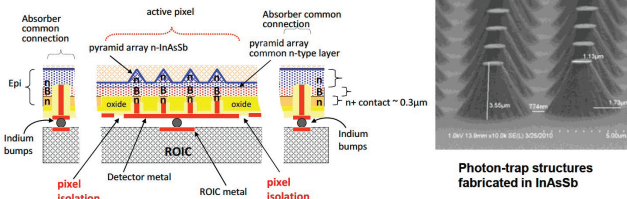


Fig. 1  $5\ \mu\text{m}$  LWIR pixels—part of a  $1280\times 1024$  array. The picture shows the indium bumps after the array has been pulled apart from a readout.

Approach uses InAsSb active layer for 10x lower volume, photon trap structures

- 10x reduction in diffusion current
- 200K operating temperature
- Broad band: 0.5 to 5  $\mu\text{m}$ , no AR coating



**Photon trap nBn and variant architectures**

Fig. 2 A photon trap structure using nBn FPAs.

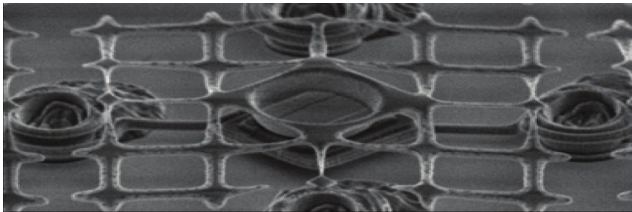


Fig. 3 Multi-band detector structure combining an LWIR microbolometer and an InGaAs visible-SWIR array.

### Photon Detectors

Photon detectors were covered in the following sessions:

- NIR/SWIR FPAs and Applications
- Air Force Infrared Research and Development
- Type II Superlattice FPAs I & II
- HgCdTe I & II
- HOT—High Operating Temperature FPAs
- Active Imaging
- QWIP and QDOT
- Posters

#### NIR/SWIR FPAs and Applications

There were ten papers in the NIR/SWIR session. This spectral region has received increasing attention in the past few years as recognition has grown of the potential to exploit night sky glow with ambient temperature FPAs—mostly InGaAs—while operating in an eye-safe band that is invisible to NIR image intensifiers.

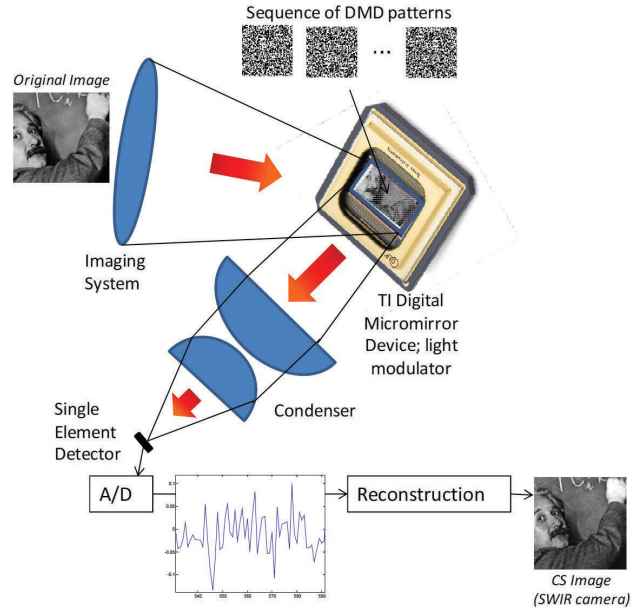


Fig. 4. Camera system for “compressed sensing” using a single-element detector and a digital micromirror array.

The first paper in this session was not SWIR-specific, but still quite interesting. A camera system—illustrated in Fig. 4—has been built using a single element detector. Rather than raster scanning the lone pixel, a digital mirror array is used to sequentially bring combinations of a number of picture elements onto the detector—presumably these represent some bases-set of the total image. This is referred to as “compressed sensing”. As the image continues to be sampled, the composite fidelity improves as illustrated in Fig. 5 which shows how the image quality changes with the percentage of samples from the full set. While this approach only needs a single detector, that fact limits it to low frame rates. The authors plan to move to small arrays to increase the frame rate.

SWIR advantages over visible in daylight conditions was illustrated—Fig. 6—for a scene taken in the Swiss alps. The visible region was limited by light scattering even on this sunny day. This is leading to imagers that

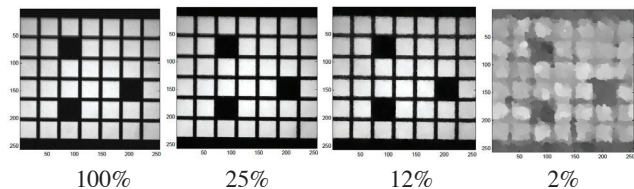


Fig. 5. Image fidelity degrades as the percentage of the full sample set is decreased.

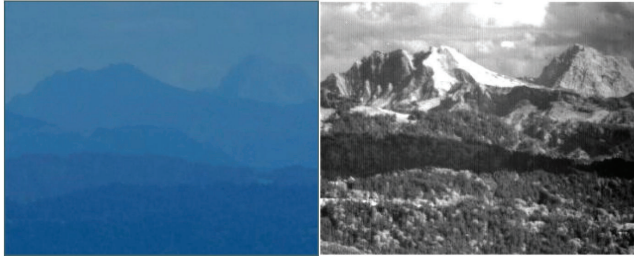


Fig. 6. Scene of the Swiss alps taken at a range of 37 km during a sunny day. Visible is shown on the left and SWIR on the right.

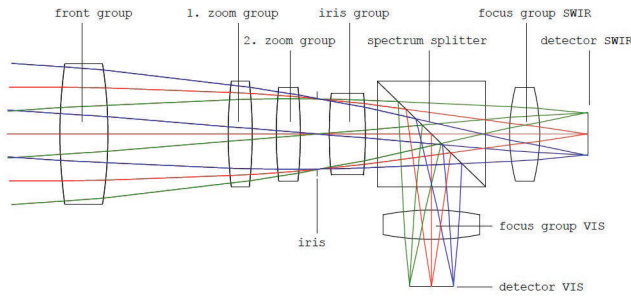


Fig. 7. Optical layout for the combined visible/SWIR imaging system.

combine both visible—HD TV— and SWIR using a beam splitter with combined fore-optics—see Fig. 7.

Coverage of the SWIR region was reported using two separate approaches in one paper. First the passivation on an MWIR sensor was modified so that it could be used all the way down to the visible region, thus covering the SWIR band. The second approach was to develop sensors based on InGaAs and progress was reported on that effort using a dual-gain readout. The InGaAs sensor substrate was thinned so that response would extend into the visible region as shown in Fig. 8. The detector dark current indicated that it was dominated by diffusion in the ambient temperature region. A solar-cell mode readout that operates the detector in

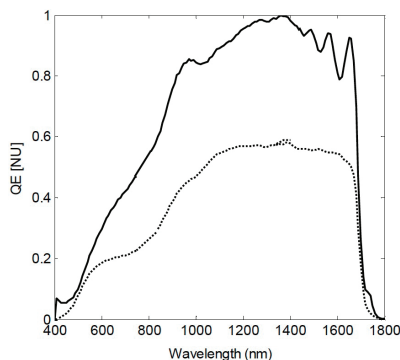


Fig. 8. Relative spectral response of a thinned InGaAs wafer with and without AR coating.

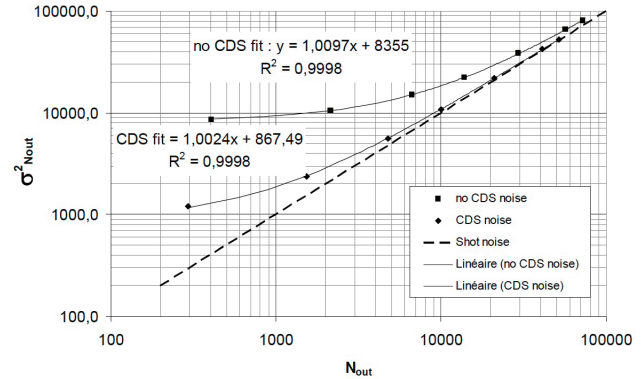


Fig. 9. Noise as a function integrated charge after CDS in high-gain mode for  $T_{int} = 130 \mu s$ ,  $V_d = -0.5 V$  at  $T \approx 30^\circ C$ . The read noise is extrapolated to 92 electrons.

forward bias, thereby logarithmically compressing the signal was described. An effective dynamic range of 120 db was claimed for this approach. The readout has been tested with a thinned InGaAs detector to allow simultaneous imaging in the visible. “Color” imaging is planned using a Bayer-like mosaic filter array. The readout also feature a direct-injection, source-follower per pixel, for operation in reverse bias.

The development of a capacitive trans-impedance amplifier (CTIA) input readout for InGaAs detector arrays was discussed. The value of correlated double sampling (CDS) was illustrated in how much closer it maintained the measured noise to the shot noise limit at low flux levels as shown in Fig. 9.

Fabrication of InGaAs on 3- and 4-inch InP substrates was described, along with test results on the diodes and imaging examples. Fig. 10 illustrates the device structure. The diode behavior as a function of bias and diode area was reported. Substrate removal to extend the response down to visible wavelengths has been achieved.

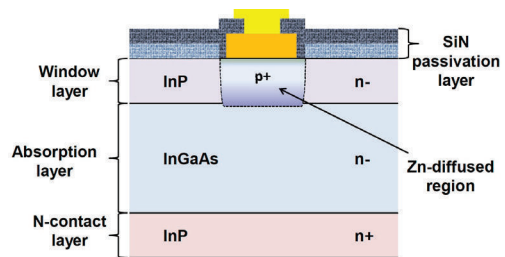


Fig. 10. Diode structure cross section showing the lightly-doped absorption layer with wider bandgap InP encapsulation/contacts. Zinc is diffused through the top InP contact to form the junction.

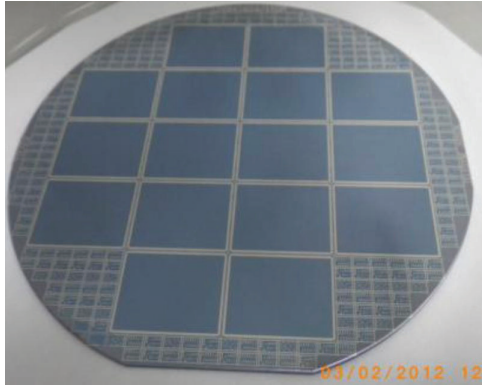


Fig. 11 A four-inch InGaAs on InP substrate wafer with sixteen 1280×1024 die. The pixel size is 15  $\mu\text{m}$ .

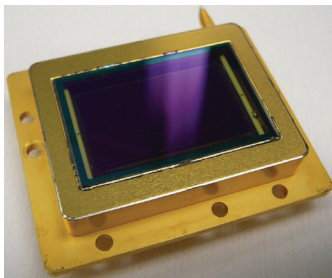


Fig. 12 A 1920×1080, 15  $\mu\text{m}$  pixel pitch, low noise InGaAs SWIR sensor with integrated thermoelectric cooler.

Large array sizes of 1280×1024 with 15  $\mu\text{m}$  pixels fabricated on 4-inch wafers was described—see Fig. 11. Pixel dimensions as small as 5  $\mu\text{m}$  are being explored in order to miniaturize SWIR cameras in the future.

Even larger InGaAs array sizes with 15  $\mu\text{m}$  pixel sizes were reported in a 1920×1080 format. A packaged die is shown in Fig. 12. An image from one of these sensors is shown in Fig. 13.



Fig. 13. Daytime imagery taken in integrate while read (IWR) mode from a 1920×1080, 15  $\mu\text{m}$  pixel pitch, low noise InGaAs SWIR sensor. The field of view of a 640×512, 15  $\mu\text{m}$  sensor is shown by the dashed box outline.

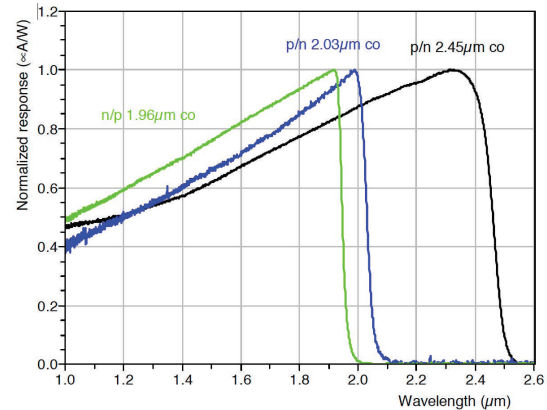


Fig. 14 Spectral response (A/W) for three HgCdTe SWIR detectors. These cutoff wavelengths are longer than those of InGaAs when that material is lattice-matched to InP substrates.

Development of a reduced power-consumption SWIR sensor without thermoelectric temperature stabilization was described. This involved calibration over the full range of operating temperature using a polynomial summation model.

A paper was presented using HgCdTe as the SWIR detector. This paper addressed longer wavelengths (see Fig. 14) than InGaAs is optimally suited to provide, and also operation at lower temperatures (60 - 160 K) and background flux levels for space sensing applications. Low dark currents were reported.

#### *Type II superlattice and nBn detectors*

Type II superlattice detectors have attracted a lot of development efforts in recent years because they potentially can out-perform HgCdTe due to theoretically longer lifetime combined with a good absorption coefficient.

In addition to Type II superlattice devices, III-V materials have been used to make a wide variety of devices that include “barriers”. These barriers are used to block the flow of majority carriers in the device, but allow the photo-excited minority carriers

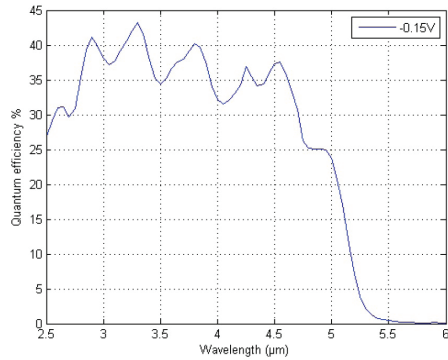


Fig. 15 Quantum efficiency for an MWIR type II superlattice detector.

to flow past the barrier to be collected. Device structures employing these barriers include nBn, pBp, pBn, etc. The absorbers in some cases are III-V alloys and in other cases Type II superlattice layers.

Papers on this topical area were found in the sessions Air Force Infrared Research and Development, the two Type II superlattice sessions, the HOT session, and in Posters.

Theoretical device structures were discussed for dual-band multispectral applications. These included structures with barrier layers.

High-energy radiation tolerance of dual-band pBp was measured for a fluence of 63 MeV protons with the sample at 80 K. Dark current increased by two orders of magnitude with 500 kRad (Si) dose. The quantum efficiency was also impacted. Some recovery was observed upon annealing at room temperature.

MWIR and LWIR Type II superlattice detectors were reported that showed significant surface current leakage indicating the need for passivation improvement. Mid-gap traps led to g-r currents at intermediate temperatures  $\sim 100$  K. The quantum efficiency of the MWIR sample was in the range of 30-40 % as shown in Fig. 15.

A 1024 $\times$ 1024 format LWIR type II superlattice was reported using the “complementary-barrier” or CBIRD structure. These devices now respond at zero bias—they no longer require a bias before generating a photoresponse. The detector array had a cutoff of 11.3  $\mu\text{m}$  and operability of 96.3%. Imaging was shown.

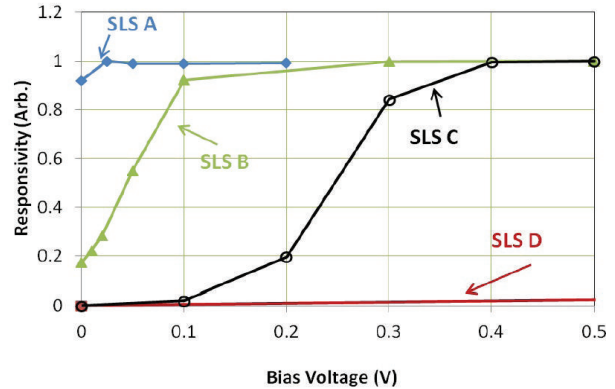


Fig. 16 Responsivity vs. bias voltage for 4 Type II SLS samples. Note that sample A gives good responsivity at zero bias.

A program to develop Type II superlattice infrared detectors for space program applications was described. Data for an MWIR single-element detector was presented.

Challenges in the effort to optimize Type II superlattice devices were reviewed. Topics addressed included:

- Device design
- Material growth
- Device processing
- Minority carrier lifetime

An example of some of the progress being made is illustrated in Fig. 16 that shows that the presence of barriers that inhibit photo-carrier collection have been reduced for sample A so that no bias is needed to overcome a barrier in order for photocurrent to flow.

A second paper demonstrated imaging with a 1024 $\times$ 1024 format LWIR type II superlattice array, in this case incorporating InSb as well as InAs and GaSb into the device structure. Quantum efficiency was reported to be in the range of 50 %. Fig. 17 shows an image taken with this array.



The optical absorption derivative was used to study how Type II superlattice energy transitions

Fig. 17 Image taken with a 1024 $\times$ 1024 LWIR Type II superlattice detector.

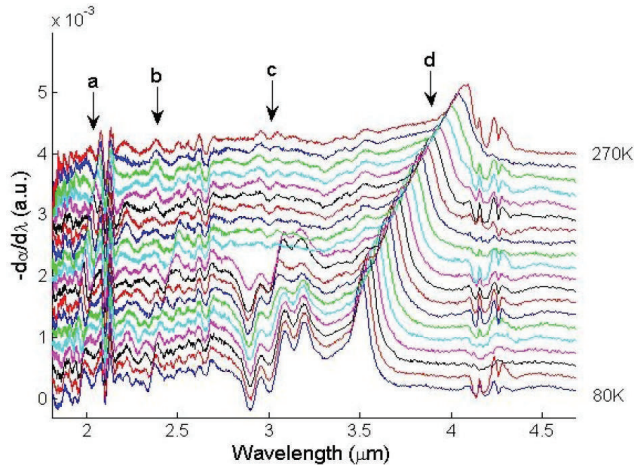


Fig. 18 Differential absorption spectra from 80 to 270 K for an MWIR Type II superlattice sample. Letters at the top note band transitions.

vary with temperature. This allowed the authors to study transitions of the higher band levels. Fig. 18 illustrates one of the measured differential spectra over the range of 80 to 270 K.

Carrier transport properties for Type II superlattice materials are another source for novel behavior not seen in conventional alloy materials. A paper was presented on the electronic transport properties using Hall effect measurements as a function of magnetic field. The authors concluded that the vertical mobility values are approximately  $5\times$  lower than the lateral value, while the carrier concentration ratio differed by  $5.5 \times 10^{-4}$ .

Passivation of Type II superlattice detectors using  $Al_2O_3$  was presented. The authors stated that this material has the lowest Gibbs free energy compared to any native oxides on the detector surface, so that its formation is preferred and stable. Experiments on MWIR material were reported.

A broad overview of developments in both Type II superlattice and pBp technologies was presented, including two-color FPA demonstrations. Fig. 19 shows the values of the noise-equivalent temperature difference (NEAT) for a two-color Type II superlattice FPA having two LWIR bands with peak response at  $7.9$  and  $10.2 \mu m$  respectively. Imagery from this FPA was also presented. A novel superlattice barrier was used in work on unipolar devices.

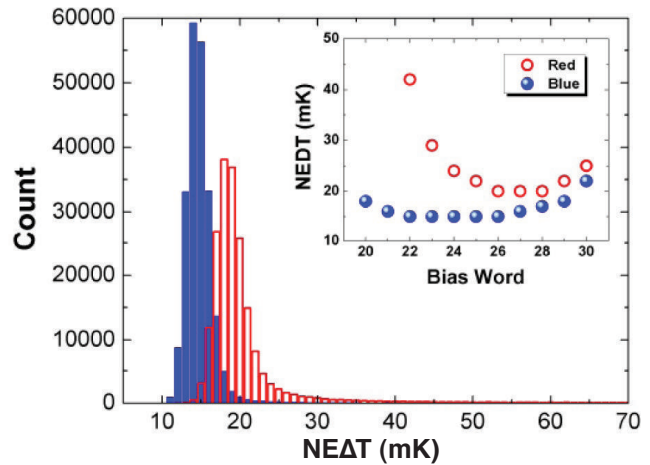


Fig. 19 NEAT histograms for two LWIR bands from a two-color Type II superlattice array in a  $640 \times 512$  format with  $30 \mu m$  pixels.

Type II superlattice material surface oxides were studied using x-ray photoelectron spectroscopy. Chlorine surface contamination was observed on dry-etched samples.

Ga-antisite defects have been suspected as the cause for short lifetimes in Type II superlattice materials. Minority carrier lifetimes up to 350 ns were measured in Ga-free  $InAs_{0.8}Sb_{0.2}$  layers at 77 K by photoluminescence decay.

Two papers were presented on efforts to increase the size of GaSb substrates to 4-inch diameter.

Tunneling current suppression in MWIR Type II superlattice detectors by employing barriers was used to allow higher doping of the absorber region in order to also suppress diffusion currents. Low NEAT values were obtained up to 130 K before the sensitivity degraded, as shown in Fig. 20.

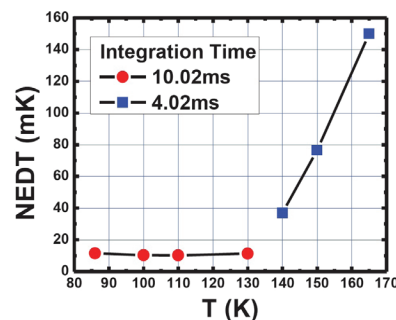


Fig. 20 Temperature dependence of NEAT for a HOT MWIR Type II superlattice FPA.

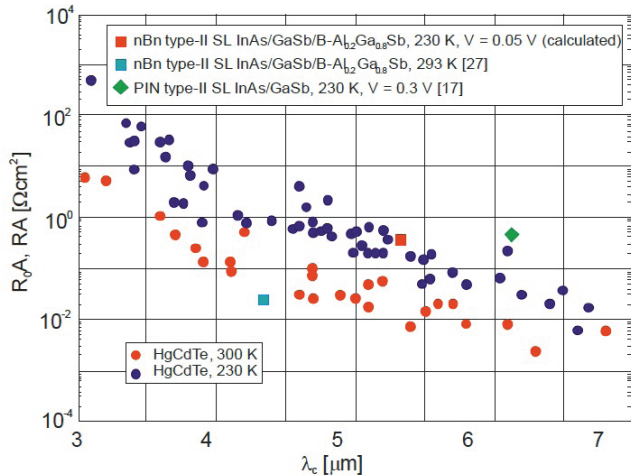


Fig. 21 Comparison of Type II superlattice and nBn MWIR detector  $R_0A$  values with those of HgCdTe at 230 and 300 K.

Type II superlattice and nBn MWIR detector dark current properties were modeled. Effective values for the temperature dependence of the trap energy responsible for trap-assisted tunneling was obtained. These traps lead to Shockley-Read-Hall (SRH) recombination that presently limit the lifetime in the III-V materials. The  $R_0A$  product of MWIR Type II superlattice and nBn detectors were compared to HgCdTe as shown in Fig. 21.

### HgCdTe detectors

The HgCdTe alloy detector—characterized by a high absorption coefficient and a long lifetime—continues to dominate the choice for a broad range of infrared applications. Aside from applications that are ideal for either InSb in the MWIR spectral band, or InGaAs in the 1.7  $\mu\text{m}$  SWIR band, or those that can utilize uncooled FPAs, HgCdTe continues to be the most popular choice. Papers in this section update how HgCdTe is continuing to develop and evolve. Papers on this topic were presented in two sessions on HgCdTe detectors as well as the HOT session and the Poster session.

A paper was presented on  $\text{Al}_2\text{O}_3$  passivation of HgCdTe using atomic-layer deposition. Films resulted in good flatband characteristics as shown in Fig. 22. The dielectric constant of the film was measured to be 7.1. Lifetime measurements increased after film deposition.

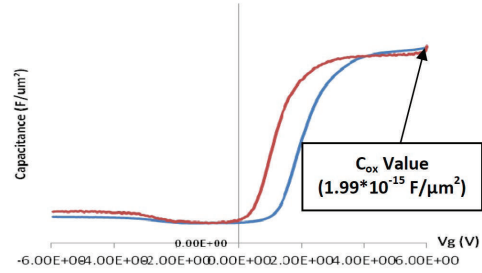


Fig. 22 C-V characteristics of  $\text{Al}_2\text{O}_3$  passivation film on HgCdTe. Flatband properties are seen near zero bias.

Mega-pixel FPAs featuring small pixels and 3-side buttable formats that can make multi-array assemblies were described. The small pixel size was demonstrated using a  $256^2$  FPA while the design of a  $1920 \times 1080$  (~2 mega-pixels) progressive scan array (see Fig. 23) with  $3.5 \times 10^6$  charge store capacity is underway.

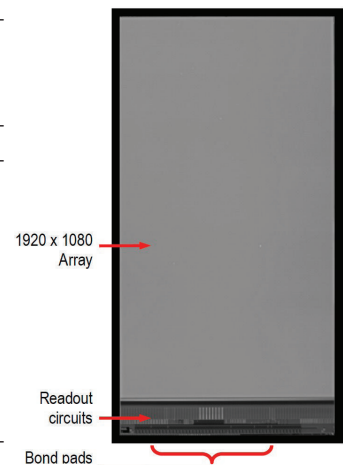


Fig. 23 Photograph of the  $1920 \times 1080$  readout for a HgCdTe MWIR array with a 3-side buttable layout and  $12 \mu\text{m}$  pixels.

The status of HgCdTe MWIR array with a 3-side buttable FPA technology in France was presented in a paper. Topics covered included crystal growth of large CdZnTe substrates, reduced pixel pitch, high-operating temperature n-on-p diodes, avalanche photodiodes, high frame-rate imaging, p-on-n devices, VLWIR arrays, and two-color arrays. Fig. 24 illustrates the projected trend in pixel size reduction.

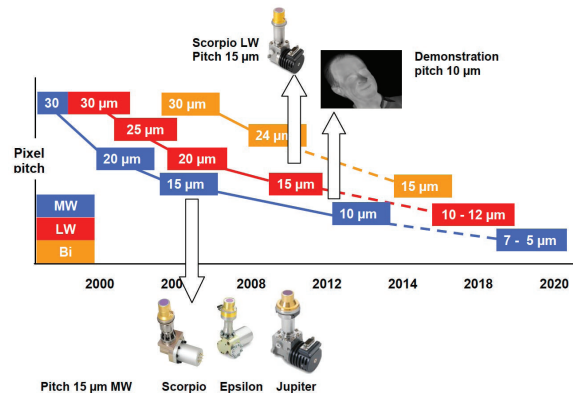


Fig. 24 Pixel size reduction trend for HgCdTe FPAs.



Fig. 25 Image taken with an LWIR HgCdTe FPA having a 1280 × 1024 format and 15 μm pixels.

In another paper, HgCdTe FPA technology developments in Germany were reviewed. Trends include smaller pixels and larger arrays, with MBE growth on GaAs substrates being explored to replace LPE material. Figure 25 is an image from with an LWIR FPA in a 1280 × 1024 format with 15 μm pitch and 12.5 × 10<sup>6</sup> charge storage capacity. The long-term reliability of HgCdTe FPAs was also established for thermal cycling and the stability of non-uniformity correction coefficients was studied.

MOVPE-grown HgCdTe for astronomy applications was featured in a paper covering SWIR and NIR spectral bands. The uniformity of x-value across a 3-inch wafer was measured to be 0.003. Mesa pixels featured optical concentration. Figure 26 shows an Arrhenius dark current plot of three n-on-p SWIR diodes. Some signal persistence was noted after signal saturation.

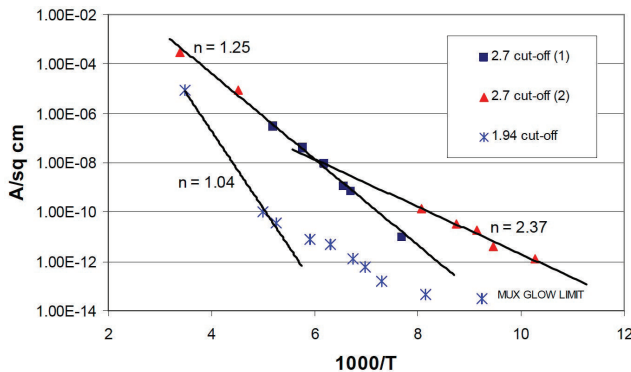


Fig. 26 Dark current vs. inverse temperature for three MOVPE-grown HgCdTe SWIR diodes.

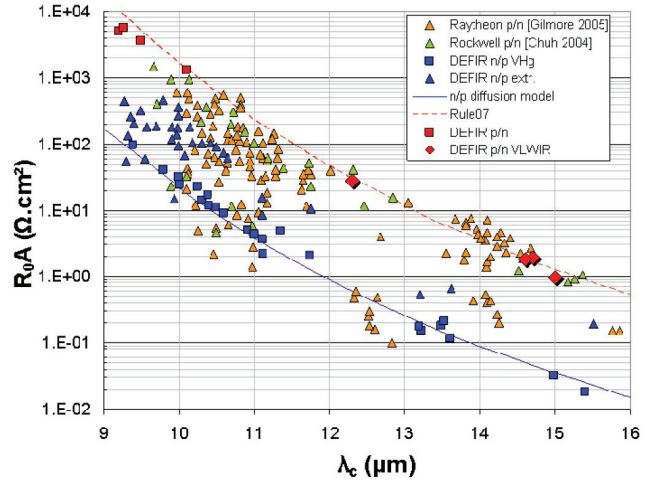


Fig. 27  $R_0A$  data at 80 K for HgCdTe photodiodes as a function of cutoff wavelength over the LWIR-VLWIR bands.

VLWIR HgCdTe p-on-n detector technology was reviewed. Junctions were formed by As ion-implantation into In-doped absorber layers grown by LPE. Fig. 27 was shown to illustrate the range of performance in terms of  $R_0A$  vs. detector cutoff wavelength.

The dark current of N+p HgCdTe photodiodes grown on GaAs substrates by MOVPE was modeled. The current was fit to a model that included an ionized donor flaw. Fig. 28 illustrates the measured data and the fit using the model. The p-type absorber layer was doped with As.

HgCdTe FPAs with photon-trapping pixels that reduce detector volume while maintaining high quantum efficiency were described with the goal of improving high operating temperature performance. A variety of volume-reducing designs were experimentally studied. An example is illustrated in Fig. 29 that shows a few pixels from an array of 512<sup>2</sup> pixels.

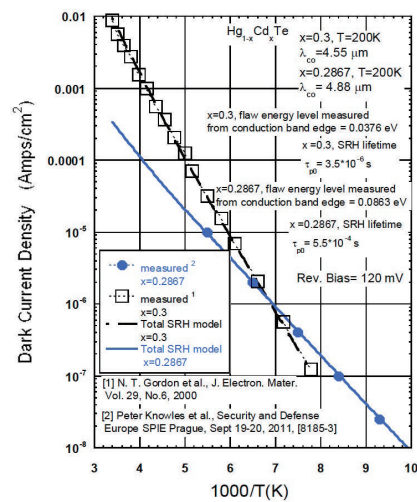


Fig. 28 Dark current vs. inverse temperature for two MWIR HgCdTe grown on GaAs substrates—measured and modeled.

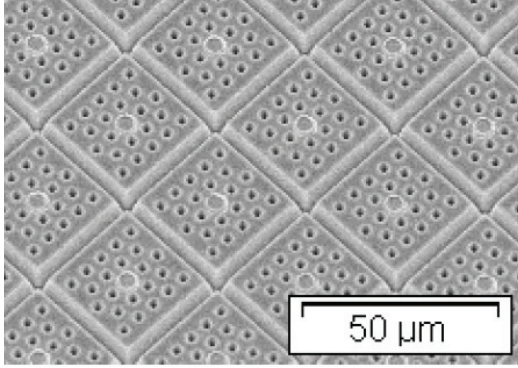


Fig. 29 30  $\mu\text{m}$  pixels with a sub-array of  $5 \times 5$  photonic-crystal holes to reduce the volume of active HgCdTe material.

### HOT—High Operating Temperature FPAs

The goal of increasing the operating temperature of FPAs without sacrificing performance is motivated by the reduction in cooler power, improved cooler efficiency, smaller size, and lighter weight sensor systems that this makes possible. This goal is being pursued using HgCdTe, Type II superlattice, and nBn materials.

The benefits of HOT performance were quantified in a paper on MWIR HgCdTe array performance. Fig. 30 shows how the cool-down time and cooler power are reduced with increasing operating temperature. Limitations to raising the operating temperature come from increasing dark current that increases NE $\Delta$ T and from an increasing percentage of defective pixels as illustrated in Fig. 31. The effect of coldshield radiation at higher operating temperatures was also noted.

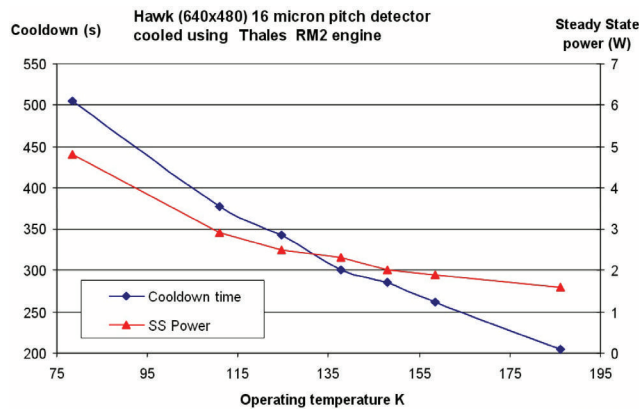


Fig. 30 Cool-down time and steady-state cooler power as a function of operating temperature for a  $640 \times 480$  HgCdTe FPA.

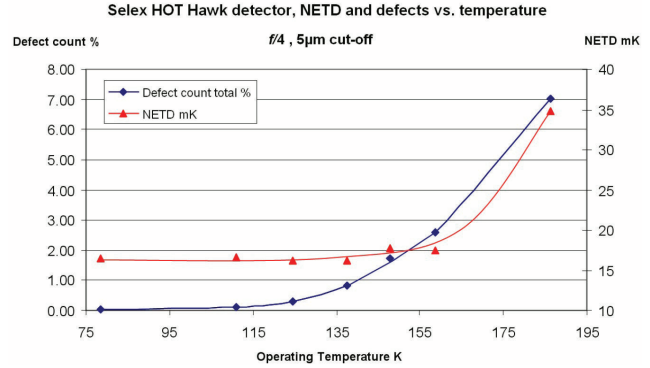


Fig. 31 NE $\Delta$ T and pixel defect percentage as a function of operating temperature for a  $640 \times 480$  HgCdTe FPA.

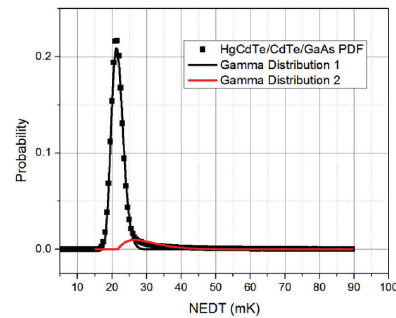


Fig. 32 NE $\Delta$ T histogram from a HgCdTe FPA grown on GaAs that is fit with two gamma functions.

HgCdTe grown on CdZnTe, Si, and GaAs were compared to InSb at elevated operating temperatures. A formalism was presented to describe the normal distribution of pixels and the distribution of high-noise pixels using two gamma functions as illustrated in Fig. 32 for a HgCdTe grown on GaAs sample.

Epitaxial InSb and XBn InAsSb detectors were discussed for HOT operation. Epitaxial growth of InSb has reduced the number of generation-recombination (g-r) centers allowing operation at 105 K with  $f/3$  optics. Fig. 33 shows the dark current reduction with epi-InSb. The XBn technology allows operation up to 175 K for material with a  $4.1 \mu\text{m}$  cutoff and total suppression of g-r currents.

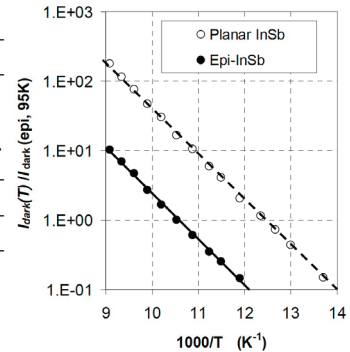


Fig. 33 Dark current of implanted InSb (planar) compared to epitaxial-grown junction material.

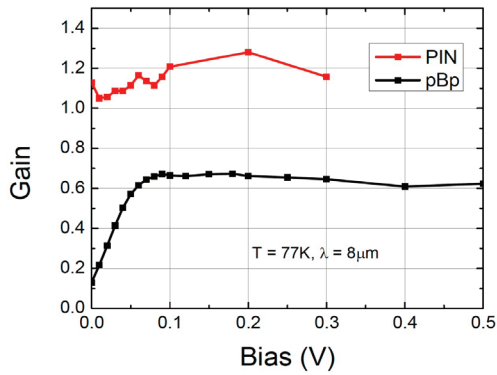


Fig. 34 Photoconductive gain of a pBp detector compared to a PIN diode, both with a Type II superlattice absorber.

The photoconductive gain for a pBp device was compared to that of a PIN diode. Both devices used Type II superlattice absorbers. Fig. 34 shows the measured gain. It was conjectured that the gain of the pBp device was limited by the short lifetime and low bias voltage in the neutral absorber region.

Numerical 3D modeling of nBn devices was described for InAs back-side illuminated  $3 \times 3$  pixel array structures. One of these included only the contact layer mesa, while the other had a mesa that include both the contact and the barrier layers of the device. It was pointed out that laying out a numerical mesh for the modeling is very critical—an example of the mesh is shown in Fig. 35. Crosstalk was calculated—a critical concern because the absorber layer is not delineated in the structures. The calculations illustrated a possible explanation for anomalously long lateral collection lengths.

An improved dry-etching process was described in connection with processing LWIR complementary-barrier (CBIRD) devices.

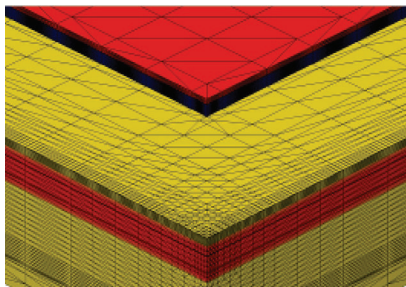


Fig. 35 Corner of the  $3 \times 3$  array of the contact plus barrier mesa pixels. The mesh layout is illustrated in the figure.

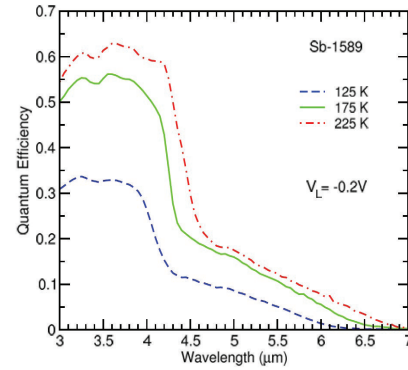


Fig. 36 Extended spectral response from InSb quantum dots in a CBIRD detector.

Quantum dots were combined with a complementary-barrier (CBIRD) detector for high operating temperature applications. The quantum dots of InSb were incorporated in order to extend the wavelength beyond the  $4.2 \mu\text{m}$  where InAsSb is lattice matched to a GaSb substrate. Figure 36 shows the extended wavelength tail that was obtained at three temperatures.

InAsSb, adjusted to a cutoff of approximately  $5 \mu\text{m}$  at 200 K, was fabricated with a backside pyramid structure to facilitate minimal reflection. This led to high quantum efficiency, as illustrated in Fig. 37.

HOT operation was pursued using p<sup>+</sup>n HgCdTe detectors for both MWIR and LWIR spectral bands. For the LWIR band— $9.3 \mu\text{m}$  cutoff at 80 K—dark current was two orders of magnitude lower for p<sup>+</sup>n compared with a standard n<sup>+</sup>p structure. This allowed the operability to be maintained above 99 % up to 110 K as shown in Fig. 38.

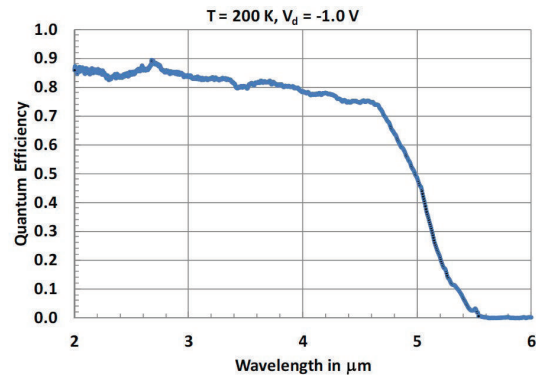


Fig. 37 High quantum efficiency achieved in an InAsSb detector with anti-reflection backside pyramids.

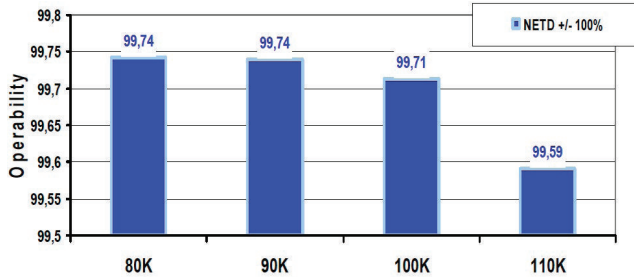


Fig. 38 Operability of LWIR (9.3  $\mu\text{m}$  @ 80 K) HgCdTe p+n detectors remains above 99 % up to 110 K.

### Active Imaging

Presentations in active imaging included both InGaAs and HgCdTe FPAs operating in the SWIR spectrum.

APDs (avalanche photodiodes) with impact ionization engineering ( $I^2E$ ) structures based on InAlAs and InGaAlAs heterostructures as avalanche layers have achieved an excess noise factor of 0.15 and a noise equivalent power (NEP) of 150  $\text{fW}/\text{Hz}^{1/2}$  over 1 GHz bandwidth at 1.06  $\mu\text{m}$ . New results with APDs having multiple  $I^2E$  stages showed optical gains over 100 prior to breakdown with low excess noise. A fully functional 16 channel photoreceiver was built for a NASA LIDAR system. The NEP of one channel is shown in Fig. 39.

HgCdTe hole-avalanche APDs were reviewed in a number of array formats including linear and 2D. Operation in the linear mode for photon counting with no dead time was discussed—see Fig. 40. Detection probability was reported to be 99.6 % at a gain of 20.

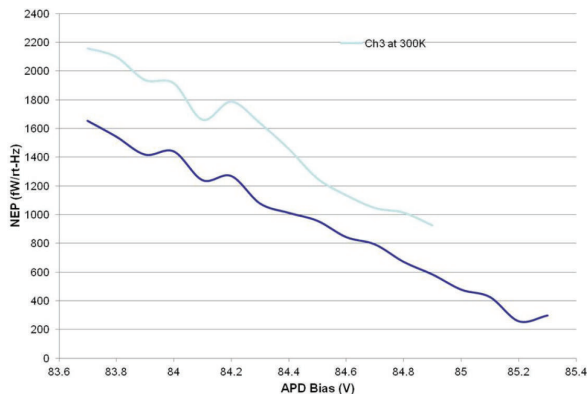


Fig. 39 Noise equivalent power for an  $I^2E$  detector channel as a function of bias.

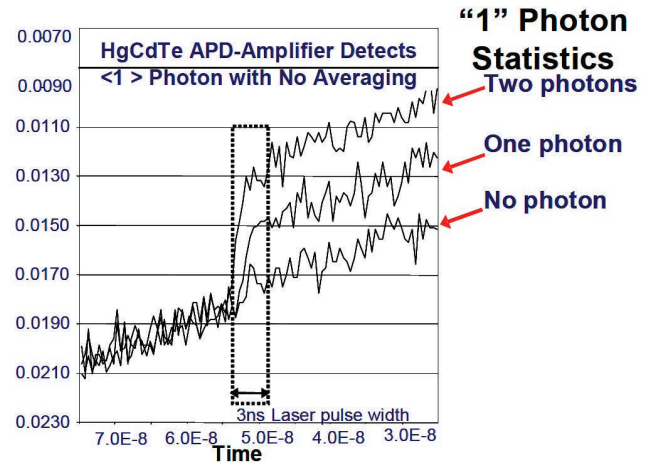


Fig. 40 Single-photon detection with a HgCdTe hole-avalanche APD detector.

Another company discussed efforts to further reduce the excess noise ( $<0.15$ ) in InGaAs SWIR APDs using a new multiplier structure based on InAlAs/InGaAlAs multiple quantum wells structures. Preliminary device characterization results show optical gain greater than 100.

A French company described development of a  $384 \times 288$  MCT e-APDs with 15  $\mu\text{m}$  pixels for both passive and 2D range gated imaging and a  $320 \times 240$  APD with 30  $\mu\text{m}$  pixels for both passive and 3D imaging.

### QWIP and QDOT

The statistical results of production history for QWIP FPAs in France were described, including NETD, operability, cooldown time, power consumption, and the stability of non-uniformity correction was reviewed. Dual-band QWIPs are now beginning production—see Fig. 41.

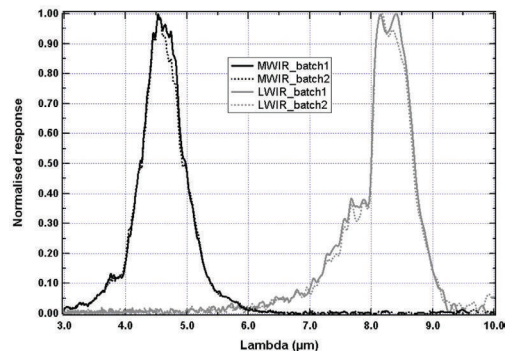


Fig. 41 Spectral responsivity for two batches of dual-band MWIR/LWIR QWIP

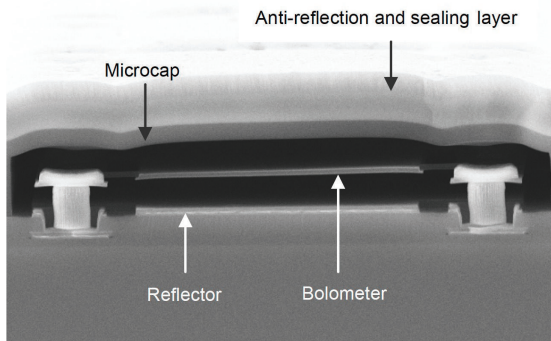


Fig. 42 Pixel-level-packaged microbolometer.

### Uncooled Thermal Detectors

The two leading uncooled technologies – vanadium oxide (VOx) and amorphous silicon microbolometers are continuing to be rapidly improved. The base line for these FPAs has become a pixel pitch of 17  $\mu\text{m}$  or less. One company described their 384  $\times$  288 amorphous silicon microbolometer that can operate TEC-less—without thermoelectric cooling—and with a power consumption of 60 mW at 60 Hz in analog mode.

Both wafer-level packaging and pixel-level packaging approaches are being developed for low-cost high-volume applications. Figure 42 shows a pixel-level-packaged pixel.

A Japanese company demonstrated a 2 M-pixel—2000  $\times$  1000—uncooled array based on series-connected Si diodes—silicon-on-insulator (SOI)—FPA with 15  $\mu\text{m}$  pixels – the largest SOI FPA fabricated to date. An SEM photo of the device is seen in Fig. 43. An image from this array is shown in Fig. 44.

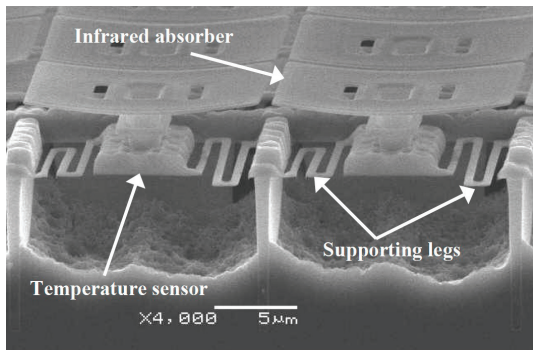


Fig. 43 SEM image of an SOI uncooled pixel structure. Each sensor contains 10 silicon diodes in series in a 15  $\mu\text{m}$  pitch.



Fig. 44 Image taken with a 2000  $\times$  1000 uncooled array fabricated with SOI technology. NE $\Delta$ T for this 15  $\mu\text{m}$  pixel array was 65 mK.

Researchers from Turkey demonstrated a simplified Non-Uniformity Correction (NUC) scheme based on pixel heating.

The development of novel uncooled detectors is also continuing. The following selected novel uncooled technologies were reported on in this conference:

- GaN as a potential material for microbolometers was investigated by growing MOCVD GaN thin films on Si (with a buffer layer) and shown to have a temperature coefficient of resistance of  $-0.64\%/^{\circ}\text{C}$ .
- A GaN micromechanical resonator was investigated as a potential uncooled infrared detector. Shifts in the resonant frequency with the absorption of infrared radiation were used as the detection mechanism.
- A “nanobolometer” in which the infrared absorption occurs in optically resonant nanoparticle arrays embedded in the gate oxide of a MOSFET device. Changes in the electric field around the nanoparticles due to the infrared induce leakage currents between the channel and the gate.

### Optics

The two IR Optics sessions, 11 and 12, addressed choice of materials for multispectral operating refractive and reflective systems, miniaturization and athermalization of optical systems, as well as applications of IR optical technologies in laboratory and field countermeasure systems.

Multi-spectral operation has proved to be the optimum solution for IR systems required to simultaneously detect and identify targets. A common aperture, common focal plane is required to answer the demand for compactness, ruggedness and ease of operation. One company discussed the selection of refractive materials for multi-spectral optical systems covering the SWIR – LWIR spectral range. When demands for athermalization and resilience are added, the number of potential refractive materials is reduced. Several design examples were presented – one of them being a catadioptric system.

Modern military optical systems for target detection, recognition, and identification often require multiple FOVs in a package that is small and light. An additional requirement may be the ability to image both the battlefield scene and a laser spot projected on a target. This spot may originate from a target range finder or designator. An army laboratory, in cooperation with industry, presented a solution for a reflective / refractive SWIR-MWIR optical system for multi FOVs – see spot operation. A unique FOV switching afocal was developed to create the three FOVs—see Fig. 45..

To protect the imager’s FPA from being damaged by excessively intense laser radiation, such as a see-spot reflected from mirror-like surfaces, a company presented their threshold-triggered blocking filter that protects the FPA during high-intensity laser irradiance and returns to normal operation as soon as the intensity is reduced to acceptable levels.

A group of scientists from industry, a governmental laboratory, and university presented an MWIR spectrometer-on-a-chip that was based on surface plasmon polaritons (SPP). The elements demonstrated included a robust, lightweight, portable spectrometer with

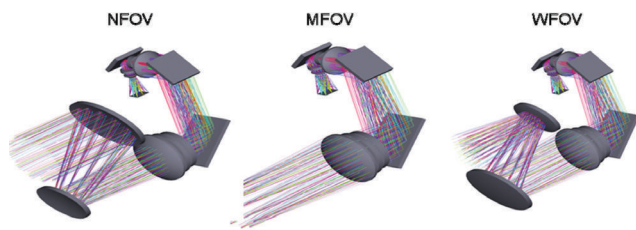


Fig. 45 Afocal and imager for the three FOVs (from left: NFOV, MFOV and WFOV)

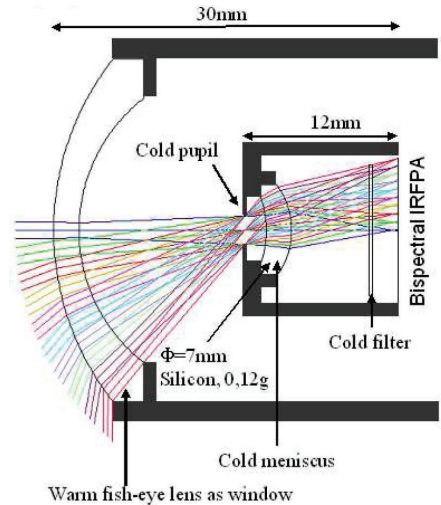


Fig. 46 Optical scheme of cooled wide FOV IR Fish-Eye camera.

no moving parts and a resolving power sufficient to enable identification of specific chemical and biological threats in the field.

Two presentations reported on successful miniaturization of optical systems by integration of the optics inside the cooled detector-dewar-cooler-assembly. Wide field of view systems, suitable for micro-UAVs, with a lens integrated in the cold shield, were discussed. FOVs between 60 and 180 degrees were obtained—see Fig. 46. Optics temperature stabilization and reduced background radiation are added advantages of these designs. A second approach, termed IR-Cam-on-Chip, integrates the optics directly on the FPA. The optical system consists of microlenses. An algorithm was developed for reconstructing a well-sampled image from a set of undersampled subimages acquired by the camera.

A companion paper reported on a very compact, fast spectrometer which operates without use of any moving parts. A wedge attached to, or part of, an FPA gives rise to an interferogram whose Fourier transform represents the source spectrum. The presentation compared the two wedge technologies – one based on grinding the FPA’s substrate to a wedge and the other based on a silicon plate attached at an angle to the front side of the FPA. The latter technology was found to be the better one.

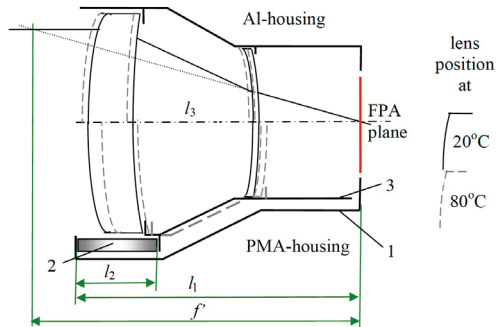


Fig. 47 Principle of passive mechanical athermalization.

Passive athermalization, which minimizes the change of focus due to variations in temperature, has become a key-technology for automotive and other outdoor applications using modern uncooled 25 and 17  $\mu\text{m}$  pitch bolometer arrays. The authors of one paper proposed a measure to quantify athermalization and discussed both optical and mechanical means for achieving best performance. A range of LWIR materials were considered and it was found that a combination of chalcogenide and crystalline optical elements, together with Passive Mechanical Athermalization, PMA—see Fig. 47—resulted in the best performance. Another presentation arrived at the same conclusion but without the use of PMA.

In the field of high and low reflectance materials, one company reported on their development of low reflectance coatings for various substrates. They concluded that multilayer coatings having Diamond Like Carbon (DLC) as a front surface coating were optimum for both MWIR and LWIR regions. Images showing the elimination of the Narcissus effect were presented. Four presentations reported on the advantages of using Visible Quality (VQ) aluminum in high reflectance IR optical systems. The properties of VQ Al were compared to those of beryllium and silicon carbide. It was concluded that excellent results are attainable using aluminum from various sources.

Among other optical technologies discussed were design trade-offs for shutters employed in man-portable infrared imagers, and photonic microstructures in the LWIR region. The micro-structures are tailored to a given transmission band and preferentially transmit a linear polarization within this band—see Fig. 48. This type of narrow-band spectro-polaric planar filter has

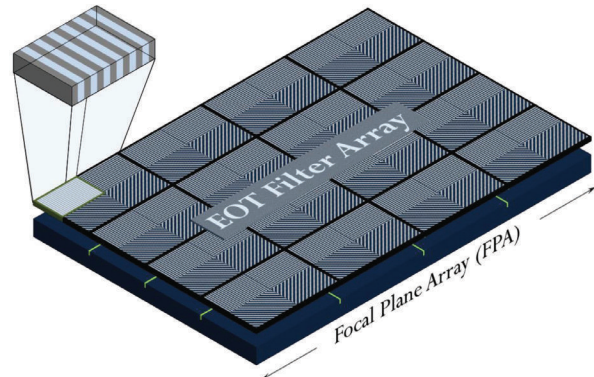


Fig. 48 Schematics of an FPA with integrated sub-pixel spectro-polarimetric transmission filters.

several applications, among them the ability to reduce false alarms in a LWIR target search system.

### Cryocoolers

Presently FPAs operating at high temperatures (HOT) of 95 – 110 K, with near-term potential for increase to up to 150 K, and having performance similar to that of their 77 – 80 K predecessors, have led to high activity among developers of FPA cryocoolers. By optimizing their cryocoolers for these higher operating temperatures, the cryocoolers, as well as the resulting infrared systems, will have higher reliability and less weight, volume and power consumption (SWaP)—see Fig. 49.

Four of the six presentations in session 10 discussed various design aspects of the HOT-compatible cryocoolers – both linear and rotary types. Two companies

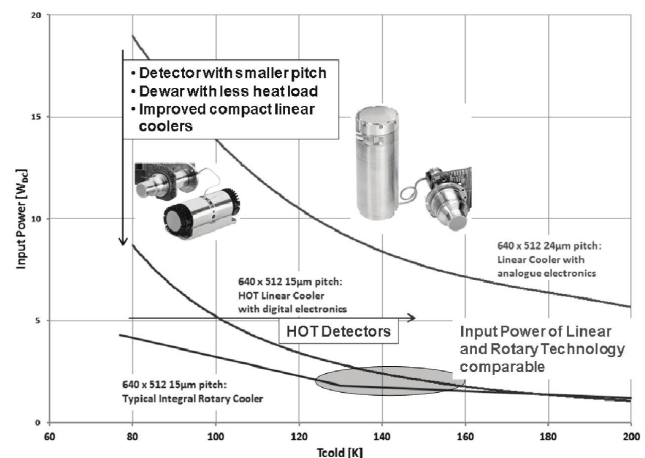


Fig. 49 Impact of detector temperature on typical power consumption.



Fig. 50 Redesigned (left) and standard (right) rotary cooler.

discussed optimization and tradeoffs for HOT rotary cryocoolers for FPA temperatures up to 200 K. The impact of the higher operational temperature on performance parameters like cooldown time, input power, Mean-Time-To-Failure (MTTF) and size—see Fig. 50—were measured and reported.

Two presentations discussed the advantages of linear cryogenic coolers for HOT FPAs. Stress was put on the miniaturization required for cryocoolers optimized for use in UAVs and by soldiers in the field—see Fig. 51. While, traditionally, rotary coolers were considered to be less expensive, lighter, more compact and normally having better electromechanical performance, this technology was claimed to be limited in terms of further SWaP reduction. A micro-miniature linear cooler was demonstrated. One company presented a compact linear cooler obtained by changing the compressor design from a dual to a single piston type. This cooler was optimized for an operating temperature of about 140 K.

As the cryocooler input power is significantly reduced for HOT conditions, the power consumption



Fig. 51 Linear compressor with regular and shortened cold fingers.

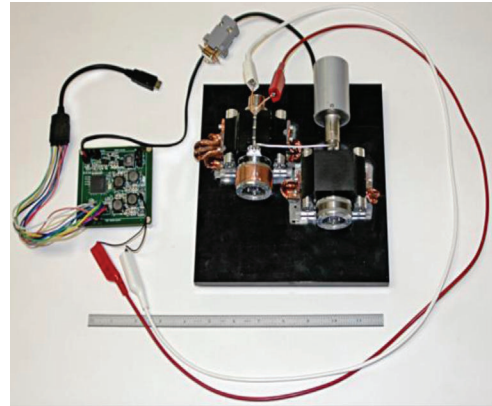


Fig. 52 Testing of a tactical cryocooler with exposed COTS Low Cost Cryocooler Electronics.

of the cooler drive and control electronics becomes relatively important. Two companies discussed design and testing of their drive electronics optimized for low input power requirements—see Fig. 52.

### Smart image and signal processing

A joint session held with conference 8355, included papers on the following topics:

- A bio-inspired system-on-chip focal plane readout architecture which at the system level, relies on an event based sampling scheme where only pixels within a programmable range of photon flux rates are output.
- A new Non-Uniformity Correction (NUC) algorithm for uncooled FPAs that needs no camera motion or registration of images. The proposed method uses a hybrid scheme including an automatic locally-adaptive contrast adjustment and a state-of-the-art image denoising method.
- An information theoretic approach for large format small pixel uncooled FPAs is used to carry out computational imaging.

A paper from conference 8355 was presented that discussed the question of how small pixels should be made—see Proceedings volume 8355.

## Applications

Presentations focusing on applications of the various infrared technologies in systems and sub-systems were presented in Sessions 2, 3 and 19. As applications are the main drivers for technology R&D, references to systems can be found throughout the Proceedings.

Hyperspectral imagers (HSI) are becoming the dominant space-based IR systems for target reconnaissance. One reason for this is that the hyperspectral data may, in some cases, allow targets to be recognized even if these targets are not spatially resolved. Obviously, these systems are required to be simple, compact and of low mass. These requirements are not well met by today's extended spectral coverage HSI systems. One laboratory suggested an HSI concept using direct imaging onto a single FPA without the use of optical dispersion elements. Two techniques were discussed. One is the use of a continuously varying band-gap instead of the discrete band-gaps used in dual-band FPAs. The other exploits the variation of a detector material's absorption coefficient with wavelength giving rise to varying "spectral photocurrents" from different depths in the material.

A national laboratory outlined the design and performance of their SWIR hyperspectral imager. The space-based system is intended for identification of natural resources. A fused silica prism is used as the dispersive element—see Fig. 53. Monitoring of background radiation and use of a smart ROIC with programmable gain are used for achieving high sensitivity from 0.9 to 2.5  $\mu\text{m}$ .

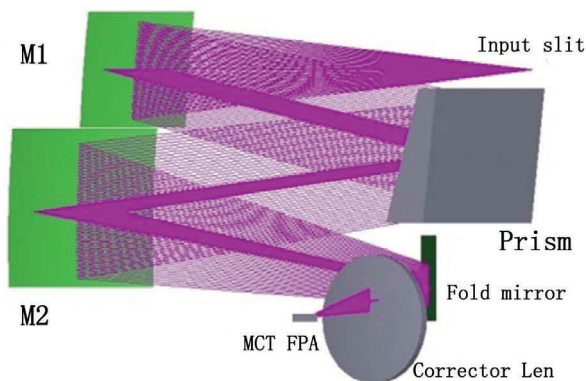


Fig. 53 SWIR spectrometer optics.

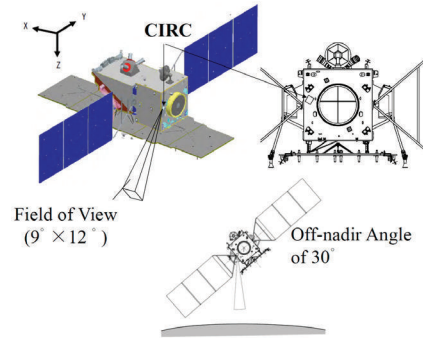


Fig. 54 Schematic view of CIRC's mounting position on a satellite.

While the HgCdTe FPA in the above system was cryogenically cooled, an aerospace exploration agency employed, for the first time, a  $640 \times 480$  pixels microbolometer in their CIRC space-based camera. The main mission of this camera is to detect wildfires. In order to increase the observation frequency, the compact camera will be mounted on several satellites. One example is shown in Fig. 54. The authors outlined the camera's design, calibration and testing.

An outline was presented of the DUCAS program. The aim of the four-year, seven nations, project is to investigate the potential benefits of combined high spatial and spectral resolution airborne imagery for several defense applications in an urban area. The program, which is based on lessons learned in Iraq and Afghanistan, includes measurements of targets and backgrounds from aerial platforms as well as ground truth observations—see Fig. 55. One important outcome of the project is to propose conceptual design of multi-function systems consisting of high resolution active and passive subsystems. A few results of the measurements were given.

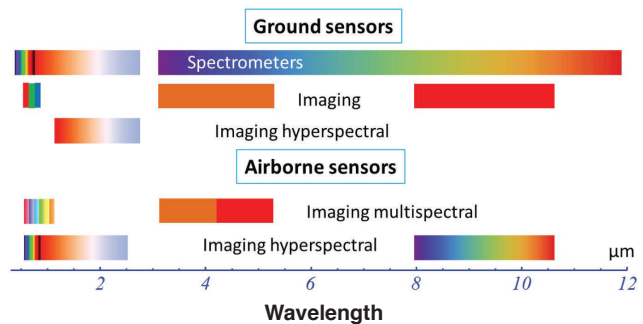


Fig. 55 Overview of ground based and airborne sensors used in data collection..

One company presented an outline of their lightweight, rugged wideband MWIR camera core designed for airborne applications. To achieve high reliability, much attention was directed toward mechanical robustness and high temperature, HOT, FPA operation. Excellent pixel operability and near-background limited performance at temperatures up to 200 K were demonstrated. Creating a common housing for the dewar and electronics was one of the many important challenges that were met.

Development of a high-volume, low-cost camera for short range security surveillance during day and night is a very attractive challenge. One company reported on their remarkable results using a camera based on their black silicon XQE technology. The camera has up to  $768 \times 480$  pixels and is sensitive in the visible and NIR parts of the spectrum. Figure 56 shows images from a room which is dark to the eye with a 940 nm LED as the only illumination.

Airborne Missile Warning Systems (MWS) are susceptible to false alarm sources such as sun glints and radiant objects with IR signature similar to that of



Fig. 56 Images collected in a completely dark room. The only illumination is from a 940 nm LED. The upper image is the XQE sensor and the lower is a standard CMOS sensor. Both sensors have  $380 \times 240$  resolution and  $11.2 \mu\text{m}$  pixels. The integration time for both is 16 msec.

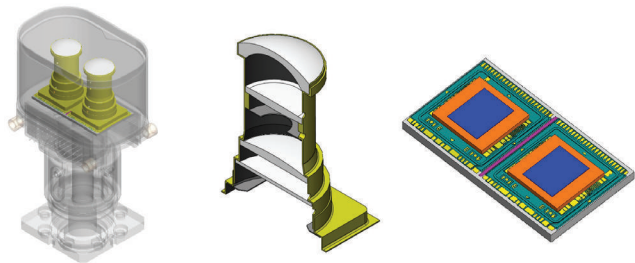


Fig. 57 Dual-color IDCA with two FPAs and two cold radiation shields and optics.

an attacking missile. One company presented their MWIR dual color sensor which effectively reduces the false-alarm-rate by comparing signals from both sides of the  $4.3 \mu\text{m}$   $\text{CO}_2$  absorption band. Each FPA has its own cold shield, which is integrated with its own optimized set of lenses and spectral filter—see Fig. 57. The reasons for using a hybrid dual color detector having two separate FPAs assembled in the same dewar instead of a monolithic dual-color type detector were explained.

Dazzling and blinding of Air-Force pilots caused by laser irradiance is a known countermeasure. One group presented their dazzling protection filter which is an efficient counter-counter-measure that reduces the high-intensity laser irradiance while retaining the transmission at wavelengths different from that of the laser. The wide-band filter returns to its earlier condition at the disappearance of the laser irradiance.

Six presentations addressed threat acquisition. The threats included terrorists at close range, vehicles and soldiers in the battlefield, poisonous gases and naval targets in littoral waters.

Facial recognition plays a crucial role in many law enforcement scenarios. One group investigated eye and full face detection when the culprit's eyes were hidden behind sunglasses or when the full face was hidden by tinted architectural and automotive glass. Both passive and active illumination were used and images collected within five SWIR bands. Marked variations in the ease of identification were observed when the center of the spectral SWIR band was varied—see Fig. 58. In a companion presentation the authors described the multi-band SWIR imager used in the investigation and determined optimum illumination, imager measurement settings, and image quality measures.

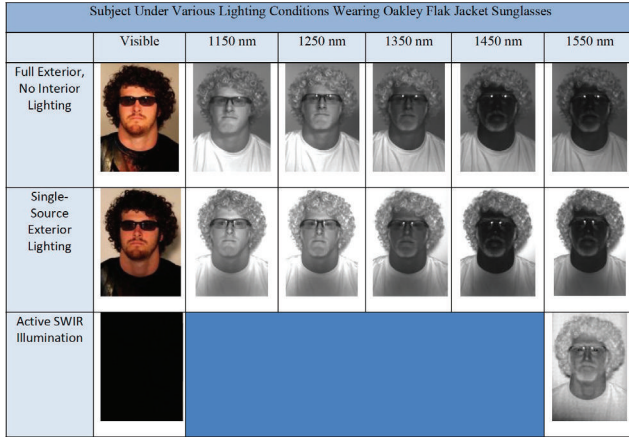


Fig. 58 Sample images for various SWIR spectral bands.

Two presentations addressed the use of thermal imagers for a driver’s vision enhancement during search for targets in a near featureless terrain. IR stereoscopic imaging, without use of goggles, is being explored as a means to increase contrast and thereby the situational awareness. One company described the two uncooled cameras, the display and the eye tracker - components used in their prototype system for the Leopard 2 tank and other vehicles. The second presentation reported on development on a stereovision camera—Fig. 59—for integration on an unmanned ground vehicle (UGV). The cameras from both companies were based on uncooled microbolometer FPAs. The possibility of obtaining range data was discussed and demonstrated.

Fourier-transform spectroscopy is used for remote detection of poisonous gases. Presently a second spectrum, the background spectrum representative of the environment, must be obtained in order to identify the gases. The collection of a good background spectrum introduces many difficulties. A university group, in cooperation with a police forensics center, has developed a method of calculating a sample spectrum without the need to acquire a background spectrum. The superiority of their robust “CSCA+SCA” method

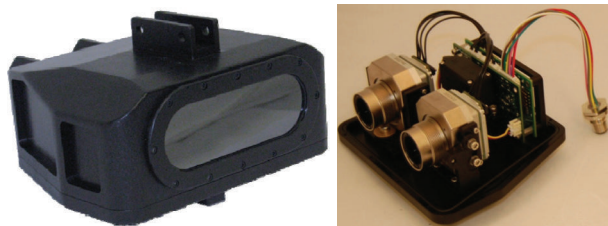


Fig. 59 Stereo camera and internal workings.

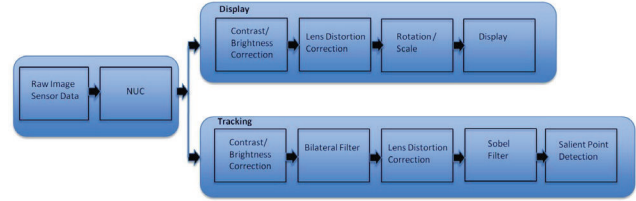


Fig. 60 Data flow schematic.

was validated by measuring the spectrum of gas-phase nitromethane – a high energetic substance more explosive than TNT.

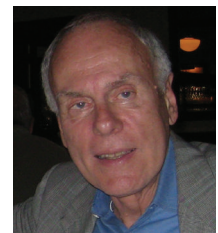
A naval IR surveillance system for detection and tracking of targets in littoral waters and at open sea is required to search a large field and, at the same time, possess a high spatial resolution for reduction of false alarms. These two requirements are difficult to satisfy in a single system. One presentation outlined the design of a single MWIR non-scanning system which covered 90° azimuth by 20° elevation. Smart image processing that reduced the false alarms and corrected for pixel non-uniformity and optical distortion was discussed—Fig. 60. Finally, some data from field experiments were presented.



Paul R. Norton



Bjørn F. Andresen



Gabor F. Fulop